

Two Loop Partition Function for Large N Pure Yang-Mills Theory on a Small S^3

Ofer Aharony^a, Joseph Marsano^b, and Mark Van Raamsdonk^c

^a*Department of Particle Physics, Weizmann Institute of Science, Rehovot 76100, Israel*

^b*Jefferson Physical Laboratory, Harvard University, Cambridge, MA 02138, USA*

^c*Department of Physics and Astronomy, University of British Columbia,
Vancouver, BC, V6T 1Z1, Canada*

We give a direct path-integral calculation of the partition function for pure 3+1 dimensional $U(N)$ Yang-Mills theory at large N on a small S^3 , up to two-loop order in perturbation theory. From this, we calculate the one-loop shift in the Hagedorn/deconfinement temperature for the theory at small volume, finding that it increases (in units of the inverse sphere radius) as we go to larger coupling (larger volume). Our results also allow us to read off the sum of one-loop anomalous dimensions for all operators with a given engineering dimension in planar Yang-Mills theory on \mathbb{R}^4 . As checks on our calculation, we reproduce both the Hagedorn shift and some of the anomalous dimension sums by independent methods using the results of hep-th/0412029 and hep-th/0408178. The success of our calculation provides a significant check of methods used in hep-th/0502149 to establish a first order deconfinement transition for pure Yang-Mills theory on a small S^3 .

1. Introduction

Pure 3+1 dimensional Yang-Mills theory on S^3 has a discrete energy spectrum which, thanks to asymptotic freedom, can be computed perturbatively for small volume. This information is encoded in the thermal partition function, which can be used to evaluate thermodynamic functions and investigate the phase structure of the theory. In this note, we explicitly compute the partition function at two-loop order in perturbation theory for the $U(N)$ Yang-Mills theory in the 't Hooft large N limit [1], by a direct evaluation of the Euclidean path integral on $S^3 \times S^1$, where the radius of S^3 is $R_{S^3} \ll 1/\Lambda_{QCD}$ and the circumference of the circle is the inverse temperature β .

Our results for the partition function may be expanded in powers of the dimensionless variable $x \equiv e^{-\beta/R_{S^3}}$ as

$$Z_{2\text{ loop}}(x) = \sum_{n=2}^{\infty} x^n (a_n + \lambda b_n \ln(x) + \mathcal{O}(\lambda^2)), \quad (1.1)$$

where a_n gives the number of states with energy n/R_{S^3} in the free theory and $b_n \lambda$ gives the sum of the order λ perturbative energy corrections for all states with energy n/R_{S^3} (λ is the 't Hooft coupling $g_{YM}^2 N$). Equivalently, $b_n \lambda$ gives the sum of one-loop anomalous dimensions for all dimension n operators in the planar Euclidean Yang-Mills theory on \mathbb{R}^4 . Using spin chain techniques, the matrix of one-loop anomalous dimensions has previously been computed in [2], so we can in principle derive the b_n 's from those results also. We find agreement between the two methods for all cases that we have checked explicitly.

As discussed in [3,4], large N $U(N)$ (or $SU(N)$) Yang-Mills theory in the limit of small volume has a Hagedorn density of states, manifested as a divergence of the partition function at a critical temperature given by $T_{c,0} = [R_{S^3} \ln(2+\sqrt{3})]^{-1}$ at $\lambda = 0$. At large (but not infinite) N , this Hagedorn divergence signals a deconfinement phase transition across which the free energy jumps from order one to order N^2 . As a physical application of our results, we can evaluate the leading perturbative correction to this critical temperature¹ by determining the point at which our two-loop partition function diverges. We find that it increases (in units of the inverse radius) as the coupling increases²:

$$T_c R_{S^3} = T_{c,0} R_{S^3} \cdot \left(1 + \frac{\lambda}{12\pi^2} + \mathcal{O}(\lambda^2) \right). \quad (1.2)$$

¹ Note that beyond first order in perturbation theory, we expect the phase transition temperature to be below the Hagedorn temperature [5], but to order λ , they are the same.

² Since the coupling runs, we should clarify that the relevant coupling is the one at the scale $1/R_{S^3}$, so an increase in the coupling is the same as an increase in $R_{S^3} \Lambda_{QCD}$.

This is consistent with the conjecture that $T_c R_{S^3}$ is monotonic in the radius, since at large radius we expect T_c to approach a constant of order Λ_{QCD} , so $T_c R_{S^3}$ is an increasing function of R_{S^3} . As another check of our results, we provide an independent calculation of the shift in T_c using a formula in [6] for the shift in the Hagedorn temperature in terms of the matrix of anomalous dimensions, which we can get from [2]. Again, we find that the two methods give the same result.

While our results are interesting in their own right, one of the main motivations for this work was to provide a check of the calculation and regularization methods used in [5] to establish that the planar Yang-Mills theory on a small S^3 undergoes a first-order deconfinement transition as the temperature is increased. That calculation involved a number of novel features related to the spherical space: sums over angular momenta instead of spatial momentum integrals, integrals over three-vector or scalar spherical harmonics on S^3 appearing in the vertices, and a novel non-gauge-invariant cutoff regularization scheme used together with counterterms chosen to restore gauge invariance in physical calculations. While the calculation in [5] had internal consistency checks, such as the cancellation of all logarithmic divergences among the diagrams, we did not have any independent method of verifying the final numerical result (the sign of which determined the order of the phase transition). Since the calculational setup and many of the steps are identical in the present calculation,³ we view the successful matching of our results here with those from other methods (involving only standard calculations on \mathbb{R}^4) as a satisfying check of the validity of our formalism⁴.

The structure of the paper is as follows: in section 2, we provide the basic setup for our calculation and outline the two-loop diagrams that will be needed in order to compute the partition function. These are divergent, so we need in addition certain one-loop counterterm diagrams. In section 3, we review our regularization scheme and calculate the necessary counterterms, including a new curvature-dependent counterterm not present for flat-space calculations. In section 4, we evaluate the regularized two-loop diagrams together with the one-loop counterterm diagrams in order to get our final result for the

³ The calculation in [5] was more specific in that the necessary information was contained in specific two and three-loop contributions to the effective action for the constant mode of A_0 on $S^3 \times S^1$ after the path integral was performed over all other (massive) degrees of freedom.

⁴ In fact, the computation described in this paper helped us to find a small mistake in the original version of the calculation of [4]. This mistake did not affect the main result of [4].

partition function and, subsequently, for the one-loop correction to the Hagedorn temperature. We verify that our results are independent of the regulator used. In section 5, we verify our results by independent calculations of the Hagedorn shift and of the first several terms in the expansion (1.1) using results from [6] and [2].

2. Setup

The basic setup for our calculation is identical to that in [5], so we give only a brief summary here, referring the reader to section 2 of that paper and section 4 of [4] for more details.

We would like to calculate the thermal partition function

$$Z = \sum_i e^{-\beta E_i} = \sum_i e^{-\beta \Delta_i / R_{S^3}} = \sum_i x^{\Delta_i} \quad (2.1)$$

for pure $U(N)$ Yang-Mills theory on S^3 with radius R_{S^3} , where β is the inverse temperature, Δ_i are the dimensions of the local operators in the theory, and E_i are the energy levels. This is given by the Euclidean path integral on $S^3 \times S^1$, with the circle (compactified Euclidean time) chosen to have circumference β , of the Euclidean Yang-Mills action

$$S_{Euc} = \frac{1}{4} \int_0^\beta dt \int d^3x \operatorname{tr}(F_{\mu\nu} F^{\mu\nu}) . \quad (2.2)$$

We use a normalization in which the Yang-Mills coupling g_{YM} appears in the interaction terms in the action. To make the path integral well-defined, we need to fix a gauge and include the appropriate Fadeev-Popov determinants. For our calculation on S^3 , it is convenient to use the gauge

$$\partial_i A^i = 0, \quad \partial_t \int_{S^3} A_0 = 0 , \quad (2.3)$$

where i runs over the spatial S^3 directions. The latter condition implies that the zero-mode of A_0 on S^3 is constant in time. We denote this mode by α .

Apart from α , which has no quadratic term in the Yang-Mills action (2.2), all other modes are massive. As such, it is convenient to first integrate them out to obtain an effective action for α . As argued in [4], this effective action can only depend on the unitary matrix $U = e^{i\beta\alpha}$ (the Wilson line of the gauge field around the thermal circle, averaged over the sphere). Further, the effect of the Fadeev-Popov determinant associated with the

second gauge-fixing condition in (2.3) is to convert the measure $[d\alpha]$ in the path integral to the Haar measure $[dU]$. Thus, we obtain

$$Z = \int [dU] e^{-S_{eff}(U)} \quad (2.4)$$

where

$$e^{-S_{eff}(U)} = \int [dA'] [dc] [d\bar{c}] e^{-S_{Euc}(A', \alpha) - S_{FP}(A, c)}. \quad (2.5)$$

Here, $[dA']$ denotes the measure for the gauge fields excluding the zero mode of A_0 . The fields c and \bar{c} are ghosts and

$$S_{FP} = - \int_0^\beta dt \int_{S^3} \text{tr}(\partial_i \bar{c} \widehat{D}^i c) \quad (2.6)$$

is the ghost action (where \widehat{D}^i is a covariant derivative), introduced to represent the Fadeev-Popov determinant associated with the first gauge-fixing condition in (2.3).

2.1. Vertices and propagators

To perform the calculation, we expand all fields into modes on S^3 (we set the radius of S^3 to be $R_{S^3} = 1$ from here on as it can always be reinstated by dimensional analysis),

$$\begin{aligned} A_0(t, \theta) &= \sum_{\alpha} a^{\alpha}(t) S^{\alpha}(\theta); \\ A_i(t, \theta) &= \sum_{\beta} A^{\beta}(t) V_i^{\beta}(\theta); \\ c(t, \theta) &= \sum_{\alpha} c^{\alpha}(t) S^{\alpha}(\theta), \end{aligned} \quad (2.7)$$

where S^{α} and V_i^{β} are scalar and vector spherical harmonics on S^3 , defined in appendix B (α and β represent angular momentum quantum numbers). This leads to the action in appendix A. Because the fields a^{α} and c^{α} appear only quadratically, we can integrate them out first to get an effective action involving only A^{β} and α . The final result includes a quadratic action

$$S_2 = \int dt \text{tr} \left(\frac{1}{2} A^{\bar{\alpha}} (-D_{\tau}^2 + (j_{\alpha} + 1)^2) A^{\alpha} \right), \quad (2.8)$$

a cubic interaction

$$S_3 = g_{YM} \int dt \text{tr} (i A^{\alpha} A^{\beta} A^{\gamma} \epsilon_{\alpha} (j_{\alpha} + 1) E^{\alpha\beta\gamma}), \quad (2.9)$$

and quartic interactions

$$S_4 = g_{YM}^2 \int dt \operatorname{tr} \left(-\frac{1}{2} A^\alpha A^\beta A^\gamma A^\delta \left(D^{\alpha\gamma\bar{\lambda}} D^{\beta\delta\lambda} - D^{\alpha\delta\bar{\lambda}} D^{\beta\gamma\lambda} \right) + \frac{1}{2} \frac{D^{\alpha_1\beta_1\gamma} D^{\alpha_2\beta_2\bar{\gamma}}}{j_\gamma(j_\gamma + 2)} [A^{\alpha_1}, D_\tau A^{\beta_1}] [A^{\alpha_2}, D_\tau A^{\beta_2}] \right), \quad (2.10)$$

where we have defined $D_\tau \equiv \partial_t - i[\alpha, \cdot]$, and $D^{\alpha\beta\gamma}$ and $E^{\alpha\beta\gamma}$ are integrals over products of three spherical harmonics that are defined in appendix B. Sums over all indices are implied.

There are in addition higher order vertices arising (like the second line in (2.10)) from integrating out a and c , but these do not enter in our two-loop calculation. We have also suppressed a set of vertices proportional to $\delta(0)$ which serve to precisely cancel terms proportional to $\delta(0)$ that arise in contracting two $D_\tau A$'s at equal times. As explained in [5], we can simply work with the set of interactions above, ignoring any $\delta(0)$ terms that arise.⁵

The propagator for A^α that follows from (2.8) is

$$\langle A_{ab}^\alpha(t) A_{cd}^\beta(t') \rangle = \delta^{\alpha\bar{\beta}} \Delta_{j_\alpha}^{ad,cb}(t - t', \alpha), \quad (2.11)$$

where Δ is a periodic function of time given for $0 \leq t \leq \beta$ by

$$\Delta_j(t, \alpha) \equiv \frac{e^{i\alpha t}}{2(j+1)} \left(\frac{e^{-(j+1)t}}{1 - e^{i\alpha\beta} e^{-(j+1)\beta}} - \frac{e^{(j+1)t}}{1 - e^{i\alpha\beta} e^{(j+1)\beta}} \right). \quad (2.12)$$

Here, α is shorthand for $\alpha \otimes 1 - 1 \otimes \alpha$, and a term $\alpha^n \otimes \alpha^m$ in the expansion of Δ should be understood to carry indices $(\alpha^n)^{ad} (\alpha^m)^{cb}$ in (2.11).

2.2. Regularization and counterterms

The two-loop diagrams that we are required to evaluate contain divergences, as we should expect from gauge theory in four dimensions. To deal with these, we could apply dimensional regularization, evaluating the partition function on $S^3 \times S^1 \times \mathbb{R}^d$, and using a modified minimal subtraction procedure to obtain finite and gauge-independent results.

⁵ These $\delta(0)$'s are related to our choice of Coulomb gauge, which leads to singular propagators for A_0 and the ghosts. In appendix D, we explain a more well-defined way of performing Coulomb-gauge calculations which avoids any $\delta(0)$ terms in the calculation but nevertheless gives the same results, justifying our naive cancellations.

In practice, to overcome technical difficulties with this regularization scheme, we will use the regularization scheme of [5] involving momentum cutoffs, which requires adding to the action counterterms designed to yield results that are completely equivalent to those of dimensional regularization.⁶ This is reviewed in detail in section 3. For our calculation, the counterterm vertices that contribute are⁷

$$\begin{aligned}
S_{ct} &= \lambda \int_0^\beta dt \int_{S^3} \text{tr} \left(A_i^{SU(N)} (Z_0 - Z_1 \partial_j^2 - Z_2 D_\tau^2) A_i^{SU(N)} \right) \\
&= \lambda \int_0^\beta dt \text{tr} \left(A^{\bar{\alpha}} (Z_0 + Z_1 (j_\alpha + 1)^2 - Z_2 D_\tau^2) A^\alpha \right) \\
&\quad - \frac{\lambda}{N} \int_0^\beta dt \text{tr} (A^{\bar{\alpha}}) (Z_0 + Z_1 (j_\alpha + 1)^2 - Z_2 D_\tau^2) \text{tr} (A^\alpha),
\end{aligned} \tag{2.13}$$

where $\lambda \equiv g_{YM}^2 N$ and Z_i are regulator dependent constants that we will determine in section 3.

2.3. One loop result

The evaluation of the partition function at one-loop order has been carried out in [4]. The result is

$$Z_{1\text{-loop}} = \int [dU] e^{-S_{1\text{-loop}}^{\text{eff}}(U)}, \tag{2.14}$$

where

$$S_{1\text{-loop}}^{\text{eff}}(U) = - \sum_{n=1}^{\infty} \frac{1}{n} z(x^n) \text{tr}(U^n) \text{tr}(U^{\dagger n}), \tag{2.15}$$

and we define

$$z(x) \equiv \frac{6x^2 - 2x^3}{(1-x)^3} \tag{2.16}$$

which is the single mode partition function for a free vector field on S^3 . The unitary matrix integral can be evaluated explicitly at large N to give [4]

$$Z_{1\text{-loop}} = e^{-\beta F_{1\text{-loop}}} = \prod_{n=1}^{\infty} \frac{1}{1 - z(x^n)}. \tag{2.17}$$

⁶ More precisely, the results are equivalent to dimensional regularization in a gauge where $3+d$ components of the gauge field participate in the Coulomb gauge condition (2.3). This is related to the more general approach of split-dimensional regularization [7,8,9,10], in which the number of degrees of freedom that do not participate in the Coulomb gauge condition is also varied.

⁷ As indicated, it is only the $SU(N)$ part of the gauge field $A_i^{SU(N)} \equiv A_i - \frac{1}{N} \text{tr}(A_i)$ that can be present in the counterterms since the $U(1)$ part of the theory is free.

The function z increases monotonically from 0 to ∞ as x increases from 0 to 1 (i.e. as the temperature increases from 0 to ∞), so the $n = 1$ term in the product leads to a divergence as the temperature is increased to the critical value $x_{c,0}$ such that $z(x_{c,0}) = 1$, or

$$T_{c,0}R_{S^3} = (\ln(2 + \sqrt{3}))^{-1} \approx 0.75933. \quad (2.18)$$

This is the Hagedorn temperature of the large N free theory (and of the interacting theory in the small volume limit). For higher temperatures (at finite N) there is a different saddle point dominating the path integral, and Z behaves as $\exp(-\beta N^2 f(T))$.

2.4. Two loop calculation

At two-loop order, the partition function is given by

$$Z_{2\text{-loops}} = \int [dU] e^{-S_{1\text{-loop}}^{\text{eff}}(U) - S_{2\text{-loop}}^{\text{eff}}(U)}, \quad (2.19)$$

where

$$\begin{aligned} e^{-S_{2\text{-loop}}^{\text{eff}}} &= \langle e^{-S_{\text{int}}} \rangle_{2\text{-loop}} \\ &= \exp\left(-\langle S_4 \rangle + \frac{1}{2}\langle S_3 S_3 \rangle - \langle S_{ct} \rangle\right). \end{aligned} \quad (2.20)$$

Here, the expectation values are evaluated in the free theory with fixed α .

The correlators in (2.20) contribute to the partition function in two different ways [11]. First, as shown in [4], the planar diagrams give a contribution of the form

$$S_{pl}^{\text{eff}} = \beta g_{YM}^2 N \sum_{n=1}^{\infty} f_n(x) \text{tr}(U^n) \text{tr}(U^{\dagger n}) + \beta g_{YM}^2 \sum_{n \geq m > 0} f_{nm}(x) \{ \text{tr}(U^n) \text{tr}(U^m) \text{tr}(U^{-n-m}) + c.c. \}. \quad (2.21)$$

The three-trace terms do not contribute to the partition function at order λ , so they can be ignored. On the other hand, the double-trace terms modify the Gaussian integral (2.14) (the path integral is Gaussian in the variables $u_n = \text{tr}(U^n)/N$), and result in order λ corrections to the denominators in (2.17).

Since (2.17) is actually the sub-leading contribution to the large N free energy (the leading $\mathcal{O}(N^2)$ contribution, coming from the action evaluated on the saddle-point, vanishes here), there are also contributions at the same order arising from *non-planar* two-loop diagrams. These are independent of U (they have a single index loop) and give a temperature-dependent prefactor to the infinite product in (2.17),

$$S_{np}^{\text{eff}} = \beta g_{YM}^2 N F_2^{np}(x). \quad (2.22)$$

Thus, in terms of the functions $f_n(x)$ and $F_2^{np}(x)$ defined in (2.21) and (2.22), the final result for the two-loop partition function is

$$\begin{aligned} Z &= e^{-\lambda\beta F_2^{np}(x)} \int [dU] e^{\sum_n \frac{1}{n} (z(x^n) - \lambda\beta n f_n(x)) \text{tr}(U^n) \text{tr}(U^{\dagger n}) + \dots} \\ &= e^{-\lambda\beta F_2^{np}(x)} \prod_{n=1}^{\infty} \frac{1}{1 - z(x^n) + \lambda n \beta f_n(x)} + \mathcal{O}(\lambda^2). \end{aligned} \quad (2.23)$$

Expressed in terms of the correction to the free-energy, we have

$$\delta F = \lambda \left(F_2^{np}(x) + \sum_{n=1}^{\infty} \frac{n f_n(x)}{1 - z(x^n)} \right). \quad (2.24)$$

From (2.23), we see that the corrected partition function will diverge when

$$1 - z(x) + \lambda\beta f_1(x) = 0, \quad (2.25)$$

so we find that the critical value of x shifts by

$$\delta x_c = \lambda\beta_{c,0} \frac{f_1(x_{c,0})}{z'(x_{c,0})} \quad (2.26)$$

or, equivalently, the critical temperature shifts by

$$\delta T_c = \lambda T_{c,0} \frac{f_1(x_{c,0})}{x_{c,0} z'(x_{c,0})}. \quad (2.27)$$

It remains to evaluate $f_n(x)$ and $F_2^{np}(x)$ by evaluating the planar and non-planar two-loop diagrams plus one-loop counterterm diagrams. We do this in section 4, but first we must discuss our regularization procedure and determine the necessary counterterms.

3. Regularization and counterterms

The regularization procedure that we use was described in detail in [5], so we only summarize it briefly here. The central idea is to cut off angular momentum sums in such a way that our calculations are as simple as possible. Such a scheme will in general break gauge and Lorentz invariance but, by choosing the right set of local counterterms in the action at the cutoff scale M , we can ensure that both are restored in the theory far below the cutoff. Specifically, we will choose counterterms so that the results for any

correlator match precisely, in the limit where the cutoff is removed, with those obtained using dimensional regularization.

Though it would be conceptually simpler to perform our calculations directly in dimensional regularization, this presents technical challenges for the required diagrams that we have not been able to overcome. On the other hand, determining the appropriate set of counterterms to ensure the equivalence of a more general cutoff scheme with dimensional regularization requires, at least to low orders in perturbation theory, the evaluation of only a few simple diagrams using both methods and a comparison of the results.

The regulator that we employ requires the insertion of a damping factor $R(\sqrt{p^2/M^2})$ for each A_i propagator, where $p^2 = p_i p_i$ ($i = 1, 2, 3$) is the magnitude of the spatial momentum and R is a function satisfying $R(0) = 1$, $R'(0) = 0$, and $R(x \rightarrow \infty) = 0$ ⁸. The regulator preserves rotational invariance, but breaks Lorentz and gauge-invariance, so we should include all possible counterterms which are local, rotationally invariant, and have dimension four or less. Since all counterterms will be at least of order λ , only quadratic counterterms (giving rise to one-loop diagrams) can contribute to the partition function at order λ . Moreover, only the A_i propagators are temperature-dependent with our choice of gauge. Thus, only the counterterms appearing in (2.13) can contribute to our result⁹.

In order to determine the constants Z_0 , Z_1 , and Z_2 , we need to evaluate at least three simple one-loop correlators to which Z_0 , Z_1 and Z_2 contribute in different linear combinations, and choose the Z 's so that the results match with the same correlators evaluated in dimensional regularization, with a minimal subtraction scheme to be described below.

It is important to note that for our calculation on the sphere, the Z_0 counterterm actually combines three separate local covariant structures,

$$\int d^4x \sqrt{g} \left(Z_0^{flat} \text{tr}(A_i A_i) + Z_0' \mathcal{R} \text{tr}(A_i A_i) + Z_0'' \mathcal{R}_{ij} \text{tr}(A_i A_j) \right), \quad (3.1)$$

the last two involving the Ricci scalar and Ricci tensor built from the metric. If Z_0' or Z_0'' are nonzero, the $\text{tr}(A_i A_i)$ counterterm on the sphere will be different than the one in flat

⁸ Note that we do not use a regulator for A_0 or ghost lines, which we have already integrated out explicitly. As described in appendix D, the cancelling $\delta(0)$ terms that appear in integrating out these fields are not physical UV divergences and may be regulated by choosing a more general gauge.

⁹ Note that a possible term of the form $\partial_i A_i \partial_j A_j$ will not contribute due to the Coulomb gauge choice.

space, with coefficients proportional to $1/R_{S^3}^2$ in addition to the flat space coefficient Z_0^{flat} proportional to M^2 . Thus, it is important that the calculation used to determine Z_0 be performed on the sphere, as we will do in section 3.2.

On the other hand, the counterterms involving Z_1 and Z_2 are already dimension 4 operators, so there is no allowed structure involving the spatial curvature that reduces to these. Consequently, it is enough to study flat-space correlators to determine Z_1 and Z_2 , and we turn to this presently.

3.1. Curvature-independent counterterms

The Z_1 and Z_2 counterterms were already determined in [5], but for completeness, we review the essential parts of that calculation here. As we suggested above, it is simplest to determine the curvature-independent counterterms by a flat space calculation. To determine Z_1 , we will compute

$$\langle A_i(0, p) A_j(0, -p) \rangle_{p^2 \delta_{ij}}^{1PI} \quad (3.2)$$

i.e. the term proportional to $p^2 \delta_{ij}$ in the 1PI two-point function of A_i , while to determine Z_2 , we will compute

$$\langle A_i(\omega, 0) A_j(-\omega, 0) \rangle_{\omega^2}^{1PI}, \quad (3.3)$$

with ω that component of the momentum which does not participate in the Coulomb gauge constraint. In each case, we compute the result (to order λ) using our regulator and the counterterm with undetermined coefficient, then repeat the calculation in dimensional regularization with a modified minimal subtraction scheme. We finally determine the counterterm by demanding that the two calculations agree.

Dimensional regularization

We will begin with the calculation in dimensional regularization. We generalize our Coulomb gauge by assuming that $3 + d$ components of the gauge field participate in the Coulomb gauge condition. With this choice, we may write the quadratic action as

$$S_2 = \int d^{d+4}x \operatorname{tr} \left\{ \frac{1}{2} \dot{A}_i \dot{A}_i + \frac{1}{2} \partial_j A_i \partial_j A_i + \frac{1}{2} \partial_i A_0 \partial_i A_0 + \partial_i \bar{c} \partial_i c \right\}. \quad (3.4)$$

The interaction terms for Euclidean Yang-Mills theory on \mathbb{R}^{d+4} in the Coulomb gauge include a cubic action

$$S_3 = g_{YM} \int d^{d+4}x \operatorname{tr} \left\{ -i \partial_i A_j [A_i, A_j] - i \dot{A}_i [A_0, A_i] + i \partial_i A_0 [A_0, A_i] - i \partial_i \bar{c} [A_i, c] \right\} \quad (3.5)$$

and quartic terms

$$S_4 = g_{YM}^2 \int d^{d+4}x \operatorname{tr} \left\{ -\frac{1}{4} [A_i, A_j]^2 - \frac{1}{2} [A_0, A_i]^2 \right\}. \quad (3.6)$$

From the quadratic action, we may derive propagators (suppressing the color indices)

$$\begin{aligned} \langle A_i(\nu, k) A_j(-\nu, -k) \rangle &\equiv \Delta_{ij}(\nu, k) = \frac{k^2 \delta_{ij} - k_i k_j}{k^2(\nu^2 + k^2)}, \\ \langle A_0(\nu, k) A_0(-\nu, -k) \rangle &= \frac{1}{k^2}, \\ \langle c(\nu, k) \bar{c}(-\nu, -k) \rangle &= \frac{1}{k^2}. \end{aligned} \quad (3.7)$$

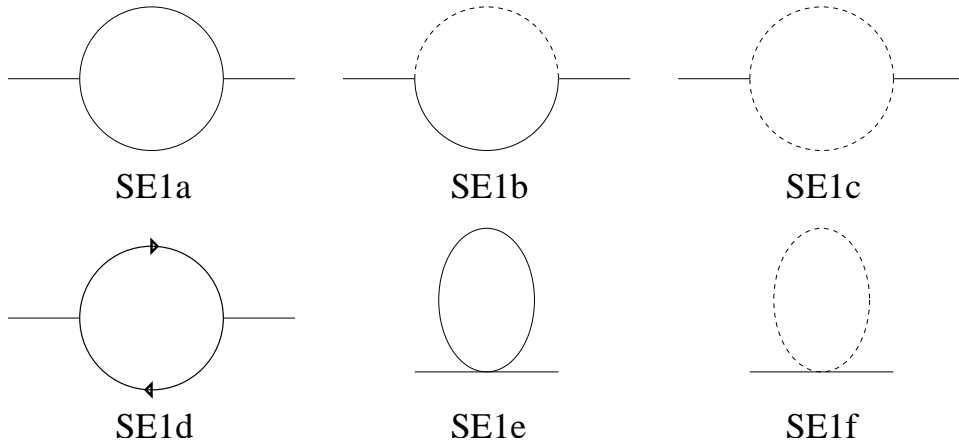


Figure 1: Diagrams that contribute to the two-point function $\langle A_i A_j \rangle$. Dashed (arrowed) lines denote A_0 (ghost) propagators, and solid lines denote A_i propagators.

The quantities (3.2) and (3.3) are both obtained from the 1PI two-point function of the gauge field. At one-loop, this gets contributions from the six diagrams of figure 1. Note, however, that diagrams SE1e and SE1f, which involve only quartic vertices, do not depend on the external momenta and hence do not contribute to (3.2) or (3.3). In addition, the A_0 loop diagram SE1c cancels with the ghost loop diagram SE1d¹⁰ so we need only focus our attention on the first two, SE1a and SE1b. For these, we find

¹⁰ Actually, these two diagrams only cancel up to a $\delta(0)$ divergence of the usual sort associated to A_0 lines. As discussed in Appendix D, this divergence is completely unphysical and is not important for any of our results.

$$\begin{aligned}
& -\frac{1}{2}\langle A_i(\omega, p)A_j(-\omega, -p)\rangle_{SE1a}^{1PI} \\
& = \int \frac{d\nu d^{d+3}k}{(2\pi)^{d+4}} \left\{ -\Delta_{ij}[(p+k)\cdot\widehat{\Delta}\cdot(p+k)] + [(p+k)\cdot\widehat{\Delta}\cdot\Delta]_i(2k-p)_j \right. \\
& \quad \left. + [(p+k)\cdot\widehat{\Delta}\cdot\Delta]_j(2k-p)_i + [(2p-k)\cdot\Delta]_i[(p+k)\cdot\widehat{\Delta}]_j + \Delta_{kl}\widehat{\Delta}_{kl}k_i(p-2k)_j \right\}, \tag{3.8}
\end{aligned}$$

where $\Delta \equiv \Delta(\nu, k)$ and $\widehat{\Delta} \equiv \Delta(\omega - \nu, p - k)$, and

$$-\frac{1}{2}\langle A_i(\omega, p)A_j(-\omega, -p)\rangle_{SE1b}^{1PI} = \int \frac{d\nu d^{d+3}k}{(2\pi)^{d+4}} \left\{ -\Delta_{ij} \frac{(\omega + \nu)^2}{(p - k)^2} \right\}. \tag{3.9}$$

It is straightforward to insert explicit expressions for the propagators and expand to order p^2 or ω^2 . In the latter case, we find¹¹

$$-\frac{1}{2}\langle A_i(\omega, 0)A_j(-\omega, 0)\rangle_{\omega^2}^{1PI} = \omega^2 \delta_{ij} \frac{d+2}{d+3} \{-I_{0,1}(0) + 2I_{0,3}(0) - 8I_{1,4}(0)\}, \tag{3.10}$$

where we define

$$\begin{aligned}
I_{m,n}(a) & \equiv \int \frac{d^{3+d}k d\nu}{(2\pi)^{4+d}} \frac{\nu^{2m} k^{2n-2m-2}}{(k^2 + a^2)(\nu^2 + k^2)^n} \\
& = \frac{a^d}{2^{4+d} \mu^d (\pi)^{\frac{5+d}{2}}} \frac{\Gamma(n - m - \frac{1}{2}) \Gamma(m + \frac{1}{2}) \Gamma(1 + \frac{d}{2}) \Gamma(-\frac{d}{2})}{\Gamma(n) \Gamma(\frac{3}{2} + \frac{d}{2})} \\
& = \frac{1}{4\pi^3} \frac{\Gamma(n - m - \frac{1}{2}) \Gamma(m + \frac{1}{2})}{\Gamma(n)} \left(\ln\left(\frac{\mu}{a}\right) + \left[\frac{1}{\epsilon} + \frac{1}{2} \ln(\pi) - \frac{\gamma}{2} + 1 \right] \right). \tag{3.11}
\end{aligned}$$

Here, μ is the regularization scale introduced, as usual, to keep $I_{m,n}(a)$ dimensionless as d is varied. In the last line, we have set $d = -\epsilon$ and expanded for small ϵ . The integrals for $a = 0$ in (3.10) contain infrared divergences in addition to the UV divergences, so rather than comparing these directly between the two schemes, we write $I(0) = I(a) + \{I(0) - I(a)\}$, and, noting that the expression in curly brackets contains no UV divergence and must agree between the two schemes, focus on the $I(a)$ term and compare this between the two schemes to determine the counterterms.

For our calculations, it is convenient to choose a minimal subtraction scheme which sets the combination in square brackets in (3.11) to zero. With this choice, the only non-vanishing contributions to (3.10) are terms proportional to $\ln(\mu/a)$ and terms for which

¹¹ We have used the fact that $k_i k_j$ inside the integral may be replaced by $k^2 \delta_{ij} / (3 + d)$ if the external momentum p is set to zero.

an ϵ in the expansion of the d -dependent coefficients multiplies the $\frac{1}{\epsilon}$ part of some $I_{m,n}$. The result for (3.3) is thus

$$-\frac{1}{2}\langle A_i(\omega, 0)A_j(-\omega, 0)\rangle_{\omega^2}^{1PI} = \omega^2\delta_{ij}\left(\frac{1}{48\pi^2} - \frac{1}{8\pi^2}\ln\left(\frac{\mu}{a}\right) + \{\text{UV finite}\}\right), \quad (3.12)$$

where the UV finite term denotes the difference between the original integral and the IR regulated version¹². Following the same steps, we find that

$$\begin{aligned} -\frac{1}{2}\langle A_i(0, p)A_j(0, -p)\rangle_{p^2\delta_{ij}}^{1PI} &= p^2\delta_{ij}\left\{-\frac{4d^2 + 22d + 20}{(d+3)(d+5)}I_{0,2}(0) + \frac{d^2 + 3d - 6}{(d+3)(d+5)}I_{1,1}(0)\right. \\ &\quad \left.-\frac{8(2+d)}{(d+3)(d+5)}I_{0,4}(0) + \frac{2d^2 + 14d + 4}{(d+3)(d+5)}I_{0,3}(0)\right\} \\ &= p^2\delta_{ij}\left(\frac{29}{240\pi^2} - \frac{1}{8\pi^2}\ln\left(\frac{\mu}{a}\right) + \{\text{UV finite}\}\right). \end{aligned} \quad (3.13)$$

Cutoffs and Counterterms

We now reevaluate the correlators using the regulated momentum integrals together with counterterms, choosing the counterterm coefficients so that the results match with those of (3.12) and (3.13). Our regularization scheme employs a cutoff only for the A_i lines, so the regulated expressions for diagrams SE1a and SE1b follow by setting $d = 0$ and replacing $\Delta_{ij}(\nu, k) \rightarrow \Delta_{ij}(\nu, k)R(k/M)$ in (3.8) and (3.9). Our results may be expressed in terms of the following basic integrals:

$$\begin{aligned} \ln\left(\frac{\mathcal{A}_n M}{\mu}\right) &\equiv \int_0^\infty dq \frac{\sqrt{q^2} R^n(q)}{q^2 + \frac{\mu^2}{M^2}}, \\ C_n &\equiv \frac{1}{4\pi^2} \int_0^\infty dq q R^n(q), \\ F_2 &\equiv \frac{1}{4\pi^2} \int_0^\infty dq q R(q) R''(q). \end{aligned} \quad (3.14)$$

Again, we start with (3.3), for which we can set $p = 0$. In this case, the contributions from (3.8) and (3.9) now include regulator factors of $R^2(k/M)$ and $R(k/M)$, respectively. Starting from (3.10) with $d = 0$, we can evaluate the integrals over ν to get

$$I_{m,n}(a) \rightarrow \frac{1}{2\pi} \frac{\Gamma(n - m - \frac{1}{2})\Gamma(m + \frac{1}{2})}{\Gamma(n)} \int \frac{d^3 k}{(2\pi)^3} \frac{1}{k(k^2 + a^2)} \quad (3.15)$$

¹² Note that this term will contain a dependence on the IR cutoff $\ln(a)$, which exactly cancels that explicitly written.

and then insert the regulators. Including also the counterterm contribution, we find

$$\begin{aligned}
-\frac{1}{2}\langle A_i(\omega, 0)A_j(-\omega, 0)\rangle_{\omega^2}^{1PI} &= \omega^2\delta_{ij}\left\{Z_2 + \int \frac{d^3k}{(2\pi)^3} \frac{1}{k(k^2 + a^2)} \left(-\frac{1}{3}R(k/M) + \frac{1}{12}R^2(k/M)\right)\right\} \\
&= \omega^2\delta_{ij}\left\{Z_2 - \frac{1}{6\pi^2} \ln\left(\frac{\mathcal{A}_1 M}{a}\right) + \frac{1}{24\pi^2} \ln\left(\frac{\mathcal{A}_2 M}{a}\right)\right\}.
\end{aligned} \tag{3.16}$$

For the other correlator (3.2), we again need a regulator factor $R(k/M)$ for the contribution (3.9) from SE1b, and this time the factor $R(k/M)R(|p-k|/M)$ for the contribution (3.8) from SE1a. It is important to take the expansion of $R(|p-k|/M)$ in powers of p into account in order to correctly obtain the terms proportional to $p^2\delta_{ij}$ in (3.8). The effect of this is trivial for logarithmic divergences as only the first term, $R(k/M)$, contributes there. However, the expression (3.8) has a quadratic divergence, for which subleading terms in the expansion become important. Working everything out carefully, we find

$$\begin{aligned}
-\frac{1}{2}\langle A_i(0, p)A_j(0, -p)\rangle_{p^2\delta_{ij}}^{1PI} &= p^2\delta_{ij}\left\{Z_1 + \int \frac{d^3k}{(2\pi)^3} \frac{1}{k(k^2 + a^2)} \left(\frac{1}{5}R(k/M) - \frac{2}{5}R(k/M)^2\right)\right\} \\
&\quad - 4\left[\int \frac{d^3k d\nu}{(2\pi)^4} \frac{k^2 k_i k_j}{(p-k)^2(k^2 + \nu^2)([p-k]^2 + \nu^2)} R(k/M)R(|p-k|/M)\right]_{p^2\delta_{ij}} \\
&= p^2\delta_{ij}\left\{Z_1 + \frac{1}{10\pi^2} \ln\left(\frac{\mathcal{A}_1 M}{a}\right) - \frac{9}{40\pi^2} \ln\left(\frac{\mathcal{A}_2 M}{a}\right) - \frac{F_2}{15} - \frac{1}{40\pi^2}\right\},
\end{aligned} \tag{3.17}$$

where the first line contains the contribution from (3.9) as well as the purely logarithmically divergent terms in (3.8) and the second line contains the only term in (3.8) for which $R(|p-k|/M)$ must be expanded in p beyond the leading order. Finally, demanding that (3.17) and (3.16) agree with (3.13) and (3.12), we must have

$$\begin{aligned}
Z_1 &= \frac{1}{8\pi^2} \ln\left(\frac{M}{\mu}\right) + \frac{1}{15}F_2 + \frac{7}{48\pi^2} - \frac{1}{40\pi^2} \ln\left(\frac{\mathcal{A}_1^4}{\mathcal{A}_2^9}\right), \\
Z_2 &= \frac{1}{8\pi^2} \ln\left(\frac{M}{\mu}\right) + \frac{1}{48\pi^2} - \frac{1}{24\pi^2} \ln\left(\frac{\mathcal{A}_2}{\mathcal{A}_1^4}\right).
\end{aligned} \tag{3.18}$$

3.2. Curvature dependent counterterm

As we discussed above, the $\text{tr}(A_i A_i)$ counterterm has a coefficient which depends on the spatial curvature, so we need to determine Z_0 by a direct calculation on S^3 , though we can work on $S^3 \times \mathbb{R}^1$ rather than $S^3 \times S^1$. Thus, to find Z_0 we compute the two-point function of a mode of A_i on the sphere, again demanding that a calculation using regulator

functions and counterterms matches with the result using dimensional regularization (this time gauge theory on $\mathbb{R}^{1+d} \times S^3$). Specifically, we will compute

$$R = \sum_{m,m',\epsilon} \langle \bar{A}^{j=1,m,m',\epsilon}(\omega=0) A^{j=1,m,m',\epsilon}(\omega=0) \rangle_{1PI}, \quad (3.19)$$

the 1PI two-point function of the lowest total angular momentum mode of A_i , summed over polarizations ϵ and angular momentum states m, m' . We begin with the calculation in dimensional regularization.

Dimensional regularization

To define the dimensionally regularized theory, we choose

$$S_{Euc} = \int d^{d+1}x d^3y \text{tr} \left(\frac{1}{4} F_{IJ} F_{IJ} \right), \quad (3.20)$$

where y are the coordinates on S^3 and x are the coordinates on \mathbb{R}^{d+1} with $d = -\epsilon$, and for simplicity we take the regularization scale μ to be unity (in units of $R_{S^3}^{-1}$),

$$\mu = 1. \quad (3.21)$$

We denote by A_a the components of the gauge field in the d directions, while A_0 and A_i denote as before the components of the gauge field in the time and sphere directions. We work in the Coulomb gauge, now extended to involve $d+3$ components¹³

$$\partial_i A_i + \partial_a A_a = 0. \quad (3.22)$$

Since the divergence of A_i is no longer set to zero, the expansion of modes on the sphere now becomes

$$\begin{aligned} A_0 &= \sum_{\alpha} a^{\alpha} S^{\alpha}, \\ A_a &= \sum_{\alpha} \mathcal{A}_a^{\alpha} S^{\alpha}, \\ A_i &= \sum_{\beta} A^{\beta} V_i^{\beta} + \sum_{\alpha} \frac{1}{j_{\alpha}(j_{\alpha}+2)} \partial_a \mathcal{A}_a^{\alpha} \partial_i S^{\alpha}. \end{aligned} \quad (3.23)$$

¹³ For this part of the calculation, it is actually much simpler to choose a gauge for which only the sphere components of the gauge field participate in the Coulomb gauge condition, but we must make the present choice to be consistent with the conventions of [5] and of the previous subsection, used to compute Z_1 and Z_2 .

Note that the Coulomb gauge condition determines the coefficients of ∇S in the expansion of A_i in terms of the \mathcal{A}_a modes. With these expansions, we find that the quadratic action may be written as

$$\begin{aligned}
S_2 = \int dt d^d x \text{tr} & \left(\frac{1}{2} A^\alpha (-\partial_t^2 - \partial_a^2 + (j_\alpha + 1)^2) A^\alpha \right. \\
& + \frac{1}{2} a^\alpha (-\partial_a^2 + j_\alpha(j_\alpha + 2)) a^\alpha \\
& \left. + \frac{1}{2} \mathcal{A}_a^\alpha (-\partial_t^2 - \partial_c^2 + j_\alpha(j_\alpha + 2)) (\delta^{ab} - \frac{\partial_a \partial_b}{j_\alpha(j_\alpha + 2)}) \mathcal{A}_b^\alpha \right). \tag{3.24}
\end{aligned}$$

From these, we determine the propagators to be

$$\begin{aligned}
\langle a^\alpha(\omega, k) a^\beta(\tilde{\omega}, \tilde{k}) \rangle &= (2\pi)^{d+1} \delta(\omega + \tilde{\omega}) \delta^d(k + \tilde{k}) \frac{\delta^{\alpha\bar{\beta}}}{k^2 + j_\alpha(j_\alpha + 2)}, \\
\langle A^\alpha(\omega, k) A^\beta(\tilde{\omega}, \tilde{k}) \rangle &= (2\pi)^{d+1} \delta(\omega + \tilde{\omega}) \delta^d(k + \tilde{k}) \frac{\delta^{\alpha\bar{\beta}}}{\omega^2 + k^2 + (j_\alpha + 1)^2}, \\
\langle \mathcal{A}_a^\alpha(\omega, k) \mathcal{A}_b^\beta(\tilde{\omega}, \tilde{k}) \rangle &= (2\pi)^{d+1} \delta(\omega + \tilde{\omega}) \delta^d(k + \tilde{k}) \frac{\delta^{\alpha\bar{\beta}}}{\omega^2 + k^2 + j_\alpha(j_\alpha + 2)} \left(\delta^{ab} - \frac{k_a k_b}{k^2 + j_\alpha(j_\alpha + 2)} \right). \tag{3.25}
\end{aligned}$$

There are now additional interaction terms involving \mathcal{A} . For our calculation of the two-point function of A_i , we will need the cubic terms with at least one power of this field, and the quartic terms with either two or four powers of \mathcal{A} . In addition to those terms which appear for $d = 0$, listed in (A.2) and (A.3), the new terms of this form are:

$$\begin{aligned}
\mathcal{L}_{Aa\mathcal{A}} &= g_{YM} \text{tr} \left(-i \partial_0 \partial_a \mathcal{A}_a^\alpha [a^\beta, A^\gamma] \frac{C_{\beta\gamma\alpha}}{j_\alpha(j_\alpha + 2)} - i \partial_0 A^\alpha [a^\beta, \partial_a \mathcal{A}_a^\gamma] \frac{C_{\beta\alpha\gamma}}{j_\alpha(j_\alpha + 2)} \right), \\
\mathcal{L}_{AAA} &= g_{YM} \text{tr} \left(-i [A^\alpha, \partial_a A^\beta] \mathcal{A}_a^\gamma D^{\alpha\beta\gamma} + i \frac{(j_\alpha + 1)^2 - (j_\beta + 1)^2}{j_\gamma(j_\gamma + 2)} A_\alpha A_\beta \partial_a \mathcal{A}_a^\gamma D^{\alpha\beta\gamma} \right) \\
\mathcal{L}_{AAA} &= g_{YM} \text{tr} \left(2i A_a^\alpha A^\gamma \mathcal{A}_a^\beta C^{\alpha\gamma\beta} - i [\partial_b \mathcal{A}_b^\alpha, \partial_a A^\beta] \mathcal{A}_a^\gamma \frac{C^{\gamma\beta\alpha}}{j_\alpha(j_\alpha + 2)}, \right. \\
& \left. -i [A^\alpha, \partial_a \partial_b \mathcal{A}_b^\beta] \mathcal{A}_a^\gamma \frac{C^{\gamma\alpha\beta}}{j_\beta(j_\beta + 2)} - i A^\alpha \partial_a \mathcal{A}_a^\beta \partial_b \mathcal{A}_b^\gamma \frac{(j_\alpha + 1)^2}{j_\beta(j_\beta + 2) j_\gamma(j_\gamma + 2)} C^{\beta\alpha\gamma} \right), \tag{3.26}
\end{aligned}$$

and

$$\begin{aligned}
\mathcal{L}'_4 &= g_{YM}^2 \text{tr} \left(-\frac{1}{2} [A_a^\alpha, A^\beta] [\mathcal{A}_a^\gamma, A^\delta] D^{\beta\delta\lambda} B^{\alpha\gamma\bar{\lambda}} - \frac{1}{2} [A^\alpha, \partial_a \mathcal{A}_a^\beta] [\mathcal{A}_a^\gamma, \partial_b \mathcal{A}_b^\delta] D^{\alpha\gamma\lambda} \widehat{B}^{\beta\delta\bar{\lambda}} \right. \\
& \left. - \frac{1}{2} [A^\alpha, \partial_a \mathcal{A}_a^\beta] [\partial_b \mathcal{A}_b^\gamma, A^\delta] C^{\lambda\alpha\gamma} C^{\bar{\lambda}\delta\beta} - \frac{1}{2} [A^\alpha, A^\beta] [\partial_a \mathcal{A}_a^\gamma, \partial_b \mathcal{A}_b^\delta] \frac{C^{\lambda\alpha\gamma} C^{\bar{\lambda}\beta\delta}}{j_\gamma(j_\gamma + 2) j_\delta(j_\delta + 2)} \right), \tag{3.27}
\end{aligned}$$

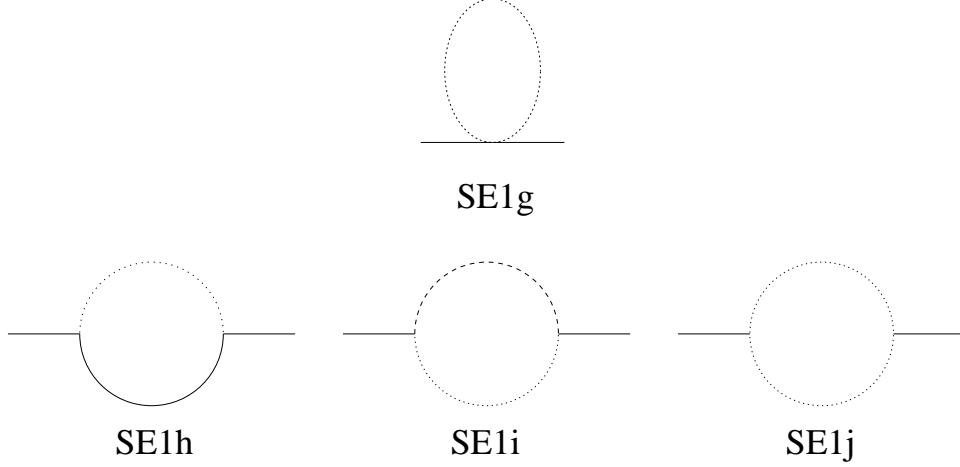


Figure 2: New diagrams with \mathcal{A}_a propagators that contribute to the two-point function $\langle A_i A_j \rangle$. Dotted (dashed) lines denote \mathcal{A}_a (a) propagators.

where B , C and \widehat{B} are defined in appendix B.

We are now ready to calculate (3.19), setting the external momentum in the d directions to zero also. In addition to the diagrams of figure 1, the new interaction terms (3.26) and (3.27) give rise to the diagrams of figure 2. Note that because the latter contain internal \mathcal{A} lines, they yield contributions to the two point function only through the multiplication of $1/\epsilon$ poles (from sums which are logarithmically divergent at $\epsilon = 0$) and prefactors proportional to ϵ .

For the n 'th diagram, we define $\Pi_n^{\alpha\beta}$ to be the correlator for two arbitrary modes A^α and A^β . This has a contribution proportional to $\delta(0)$, which we denote by δ_n (these cancel between the diagrams, and the naive cancellation may be justified by the method in appendix D), and a finite contribution. After setting $\beta = \bar{\alpha}$, choosing $j_\alpha = 1$ and summing over the external m 's and ϵ 's, we denote the finite contribution by G_n . Some useful formulae may be found in appendix C.

We begin with the diagrams involving quartic vertices. Diagram SE1e gives

$$\Pi_{SE1e} = 2(D^{\alpha\gamma\lambda}D^{\beta\bar{\gamma}\bar{\lambda}} - D^{\alpha\beta\lambda}D^{\gamma\bar{\gamma}\bar{\lambda}}) \int \frac{d\omega d^d k}{(2\pi)^{d+1}} \frac{1}{k^2 + \omega^2 + (j_\gamma + 1)^2}. \quad (3.28)$$

From this, we find

$$\begin{aligned} G_{SE1e} &= -\frac{8}{\pi^2} \frac{1}{(4\pi)^{\frac{d+1}{2}}} \Gamma\left(\frac{1}{2} - \frac{d}{2}\right) \sum_{j=1}^{\infty} \frac{j(j+2)}{(j+1)^{1-d}} \\ &= -\frac{8}{\pi^2} \frac{1}{(4\pi)^{\frac{d+1}{2}}} \Gamma\left(\frac{1}{2} - \frac{d}{2}\right) (\zeta(-1-d) - \zeta(1-d)) \\ &= \frac{4}{\pi^2} \left(\frac{1}{\epsilon} + \frac{1}{2} \ln(\pi) + \frac{1}{2} \gamma \right) + \frac{1}{3\pi^2} + \mathcal{O}(\epsilon). \end{aligned} \quad (3.29)$$

We turn next to diagram SE1f

$$\Pi_{SE1f} = -2(D^{\alpha\lambda\gamma}D^{\beta\bar{\lambda}\bar{\gamma}} + \frac{1}{j_\lambda(j_\lambda + 2)}C^{\gamma\alpha\lambda}C^{\bar{\gamma}\beta\bar{\lambda}}) \int \frac{d^d k d\omega}{(2\pi)^{d+1}} \frac{1}{k^2 + j_\gamma(j_\gamma + 2)}. \quad (3.30)$$

This gives (at order ϵ^0) a $\delta(0)$ term

$$\delta_{SE1f} = -2\delta(0)(D^{\alpha\lambda\gamma}D^{\beta\bar{\lambda}\bar{\gamma}} + \frac{1}{j_\lambda(j_\lambda + 2)}C^{\gamma\alpha\lambda}C^{\bar{\gamma}\beta\bar{\lambda}}) \frac{1}{j_\gamma(j_\gamma + 2)} \quad (3.31)$$

and no remaining finite contribution,

$$G_{SE1f} = 0. \quad (3.32)$$

We move now to diagram SE1g, which receives contributions from the four quartic interaction terms in (3.27). The first such term contributes

$$\Pi_{SE1g,1} = -2D^{\alpha\beta\lambda}B^{\gamma\bar{\gamma}\bar{\lambda}} \int \frac{d^d k d\omega}{(2\pi)^{d+1}} \frac{1}{\omega^2 + k^2 + j_\gamma(j_\gamma + 2)} \left(d - \frac{k^2}{k^2 + j_\gamma(j_\gamma + 2)} \right). \quad (3.33)$$

We find that the two terms in the integral actually cancel each other, so the net result is

$$G_{SE1g,1} = 0. \quad (3.34)$$

For the second term in (3.27) we find

$$\Pi_{SE1g,2} = -2D^{\alpha\beta\lambda}\widehat{B}^{\delta\bar{\delta}\bar{\lambda}} \int \frac{d^d k d\omega}{(2\pi)^{d+1}} \frac{k^2 j_\delta(j_\delta + 2)}{(\omega^2 + k^2 + j_\delta(j_\delta + 2))(k^2 + j_\delta(j_\delta + 2))}. \quad (3.35)$$

To evaluate this, we perform the integral over ω followed by the k integral. The resulting summand may be expanded in powers of $1/j$, and since we find an overall factor of d , the only contributing term is

$$-\frac{3d}{2\pi} \sum_j \frac{1}{(j+1)^{1-d}} \rightarrow \frac{3\epsilon}{2\pi^2} \zeta(1+\epsilon) \rightarrow \frac{3}{2\pi^2} + \mathcal{O}(\epsilon). \quad (3.36)$$

Thus, this diagram gives a net contribution

$$G_{SE1g,2} = \frac{3}{2\pi^2}. \quad (3.37)$$

From the third term in (3.27), we find

$$\Pi_{SE1g,3} = 2 \frac{C^{\lambda\alpha\gamma}C^{\bar{\lambda}\beta\bar{\gamma}}}{j_\gamma(j_\gamma + 2)} \int \frac{d^d k d\omega}{(2\pi)^{d+1}} \frac{k^2}{(\omega^2 + k^2 + j_\gamma(j_\gamma + 2))(k^2 + j_\gamma(j_\gamma + 2))}. \quad (3.38)$$

The evaluation of this is similar to the previous diagram, and we find a net contribution of

$$G_{SE1g,3} = -\frac{1}{2\pi^2}. \quad (3.39)$$

Finally, the last term in (3.27) gives no contribution.

$$G_{SE1g,4} = 0 \quad (3.40)$$

We now move to the cubic diagrams. Diagram SE1a gives

$$\Pi_{SE1a} = 9\widehat{E}^{\alpha\gamma\delta}\widehat{E}^{\beta\bar{\gamma}\bar{\delta}} \int \frac{d\omega d^d k}{(2\pi)^{d+1}} \frac{1}{\omega^2 + k^2 + (j_\gamma + 1)^2} \frac{1}{\omega^2 + k^2 + (j_\delta + 1)^2}. \quad (3.41)$$

In this case, choosing $j_\alpha = 1$ forces $j_\delta = j_\gamma$ by the triangle inequality. We find

$$\begin{aligned} G_{SE1a} &= \frac{8}{\pi^2} \frac{1}{(4\pi)^{\frac{d+1}{2}}} \Gamma\left(\frac{3}{2} - \frac{d}{2}\right) (\zeta(-1-d) + 4\zeta(1-d) - 5\zeta(3-d)) \\ &= \frac{8}{\pi^2} \left(\frac{1}{\epsilon} + \frac{1}{2} \ln(\pi) + \frac{1}{2} \gamma\right) + \frac{47}{6\pi^2} - \frac{10}{\pi^2} \zeta(3) + \mathcal{O}(\epsilon). \end{aligned} \quad (3.42)$$

Diagram SE1b gives

$$\Pi_{SE1b} = 2D^{\alpha\rho\gamma} D^{\beta\bar{\rho}\bar{\gamma}} \int \frac{d\omega d^d k}{(2\pi)^{d+1}} \left(\frac{1}{k^2 + j_\gamma(j_\gamma + 2)} - \frac{k^2 + (j_\rho + 1)^2}{(k^2 + j_\gamma(j_\gamma + 2))(\omega^2 + k^2 + (j_\rho + 1)^2)} \right). \quad (3.43)$$

The first term here gives a $\delta(0)$ term

$$\delta_{SE1b} = 2\delta(0) D^{\alpha\rho\gamma} D^{\beta\bar{\rho}\bar{\gamma}} \frac{1}{j_\gamma(j_\gamma + 2)} \quad (3.44)$$

which cancels the first term in δ_{SE1f} , while the second term gives a finite contribution

$$G_{SE1b} = -\frac{6}{\pi^2} \left(\frac{1}{\epsilon} + \frac{1}{2} \ln(\pi) + \frac{1}{2} \gamma\right) + \frac{1}{\pi^2} + \mathcal{O}(\epsilon). \quad (3.45)$$

For diagram SE1c, we find

$$\Pi_{SE1c} = -4C^{\rho\alpha\sigma} C^{\bar{\sigma}\beta\bar{\rho}} \int \frac{d\omega d^d k}{(2\pi)^{d+1}} \frac{1}{(k^2 + j_\rho(j_\rho + 2))(k^2 + j_\sigma(j_\sigma + 2))}. \quad (3.46)$$

This gives only a $\delta(0)$ contribution,

$$\delta_{SE1c} = -4\delta(0) C^{\rho\alpha\sigma} C^{\bar{\sigma}\beta\bar{\rho}} \frac{1}{j_\rho(j_\rho + 2)j_\sigma(j_\sigma + 2)} \quad (3.47)$$

with no remainder,

$$G_{SE1c} = 0. \quad (3.48)$$

The ghost loop diagram SE1d also gives only a $\delta(0)$ term

$$\delta_{SE1d} = 2\delta(0)C^{\rho\alpha\sigma}C^{\bar{\sigma}\beta\bar{\rho}}\frac{1}{j_\rho(j_\rho+2)j_\sigma(j_\sigma+2)} \quad (3.49)$$

which, together with δ_{SE1c} , cancels the second term in δ_{SE1f} .

The remaining diagrams contain internal \mathcal{A} lines, so for each of these, it is only necessary to isolate the logarithmically divergent term in the sum. From diagram SE1i, we find

$$\Pi_{SE1i} = -2\frac{C^{\sigma\alpha\lambda}C^{\bar{\sigma}\beta\bar{\lambda}}}{j_\lambda(j_\lambda+2)}\int\frac{d\omega d^d k}{(2\pi)^{d+1}}\frac{k^2}{(k^2+j_\sigma(j_\sigma+2))(\omega^2+k^2+j_\lambda(j_\lambda+2))}, \quad (3.50)$$

where we have subtracted a term which gives a $\delta(0)$ from the ω integral because it is multiplied by a k integral which vanishes for $\epsilon \rightarrow 0$. This gives a finite term

$$G_{SE1i} = \frac{1}{2\pi^2}. \quad (3.51)$$

For SE1h, we have the contribution

$$\begin{aligned} \Pi_{SE1h} &= 2D^{\alpha\rho\lambda}D^{\beta\bar{\rho}\bar{\lambda}}\left(1 - \frac{(j_\rho+1)^2 - (j_\alpha+1)^2}{j_\lambda(j_\lambda+2)}\right)\left(1 - \frac{(j_\rho+1)^2 - (j_\beta+1)^2}{j_\lambda(j_\lambda+2)}\right) \\ &\cdot j_\lambda(j_\lambda+2)\int\frac{d\omega d^d k}{(2\pi)^{d+1}}\frac{k^2}{(\omega^2+k^2+(j_\rho+1)^2)(\omega^2+k^2+j_\lambda(j_\lambda+2))}\frac{1}{k^2+j_\lambda(j_\lambda+2)}. \end{aligned} \quad (3.52)$$

This gives a finite contribution

$$G_{SE1h} = -\frac{4}{3\pi^2}. \quad (3.53)$$

Finally, we find that diagram SE1j gives a net contribution of

$$\begin{aligned} \Pi_{SE1j} &= -C^{\rho\alpha\sigma}C^{\bar{\sigma}\beta\bar{\rho}}\int\frac{d\omega d^d k}{(2\pi)^{d+1}}\frac{1}{(\omega^2+k^2+j_\sigma(j_\sigma+2))(\omega^2+k^2+j_\rho(j_\rho+2))} \\ &\cdot \{4d+2k^2(B_\alpha+B_\beta-2(E_\rho+E_\sigma)) \\ &+k^4((B_\alpha-2E_\sigma)(B_\beta-2E_\rho)-2B_\alpha E_\sigma-2B_\beta E_\rho) \\ &-k^6((B_\beta-2E_\rho)B_\alpha E_\sigma+(B_\alpha-2E_\sigma)B_\beta E_\rho)+k^8 B_\alpha B_\beta E_\rho E_\sigma\}, \end{aligned} \quad (3.54)$$

where we have defined

$$E_\rho \equiv \frac{1}{k^2 + j_\rho(j_\rho + 2)}, \quad B_\alpha \equiv \frac{j_\sigma(j_\sigma + 2) + j_\rho(j_\rho + 2) + (j_\alpha + 1)^2}{j_\sigma(j_\sigma + 2)j_\rho(j_\rho + 2)}. \quad (3.55)$$

In evaluating this, things simplify, since we take $j_\alpha = j_\beta = 1$ and this forces $j_\rho = j_\sigma$. We have, as an intermediate step,

$$G_{SE1j} = \sum_a \frac{a(a+1)^2(a+2)}{\pi^2} \int \frac{d^d k}{(2\pi)^d} \frac{1}{(k^2 + a(a+2))^{\frac{3}{2}}} \left\{ (d-1) + \left(\frac{(1 + \frac{1}{2}Bk^2)a(a+2)}{k^2 + a(a+2)} \right)^2 \right\}, \quad (3.56)$$

where

$$B \equiv 2 \frac{a(a+2) + 2}{a^2(a+2)^2}. \quad (3.57)$$

After computing the integrals, we find all terms are proportional to d . Expanding in powers of $1/a$ and keeping only $1/a^{1-d}$ terms in the summand, we find a net contribution of

$$G_{SE1j} = -\frac{11}{6\pi^2}. \quad (3.58)$$

Combining all terms, our total result is

$$G_{dimreg} = \frac{6}{\pi^2} \left[\frac{1}{\epsilon} - \frac{1}{2}\gamma + \frac{1}{2} \ln(\pi) + 1 \right] + \frac{6}{\pi^2}\gamma + \frac{3}{2\pi^2} - \frac{10}{\pi^2}\zeta(3). \quad (3.59)$$

Using the modified minimal subtraction scheme defined in §3.1, the quantity in square brackets is set to zero, so we find finally that

$$G_{dimreg} = \frac{6}{\pi^2}\gamma + \frac{3}{2\pi^2} - \frac{10}{\pi^2}\zeta(3). \quad (3.60)$$

Cutoffs and Counterterms

We now repeat the calculation using a regulator function $R(\sqrt{-\nabla^2/M^2})$. Our scheme applies this only to the A_i lines, for which $-\nabla^2$ gives $(j+1)^2$ for the mode with total angular momentum quantum number j . The expressions Π_i for the diagrams are the same as above, so we simply set $d = 0$ and insert the regulator functions. We express our results in terms of the basic integrals defined in (3.14), using the Euler-McLaurin formula to compare infinite sums with integrals.

For diagram SE1e, we find

$$G'_{SE1e} = -\frac{4}{\pi^2} \sum_{a=1}^{\infty} a R\left(\frac{a}{M}\right) + \frac{4}{\pi^2} \sum_{a=1}^{\infty} \frac{1}{a} R\left(\frac{a}{M}\right) = -16M^2 C_1 + \frac{4}{\pi^2} \ln\left(\frac{\mathcal{A}_1 M}{\mu}\right) + \frac{1}{3\pi^2} + \frac{4\gamma}{\pi^2}. \quad (3.61)$$

For diagram SE1a, we find

$$\begin{aligned}
G'_{SE1a} &= \frac{2}{\pi^2} \sum_{a=1}^{\infty} a R^2\left(\frac{a}{M}\right) + \frac{8}{\pi^2} \sum_{a=1}^{\infty} \frac{1}{a} R^2\left(\frac{a}{M}\right) - \frac{10}{\pi^2} \sum_{a=1}^{\infty} \frac{1}{a^3} \\
&= 8M^2 C_2 + \frac{8}{\pi^2} \ln\left(\frac{\mathcal{A}_2 M}{\mu}\right) - \frac{1}{6\pi^2} + \frac{8\gamma}{\pi^2} - \frac{10}{\pi^2} \zeta(3).
\end{aligned} \tag{3.62}$$

Diagram SE1b contains a $\delta(0)$ piece that is cancelled by the remaining diagrams. This leaves the result

$$\begin{aligned}
G'_{SE1b} &= -\frac{1}{\pi^2} \sum_{a=3}^{\infty} \frac{a^2-1}{a-2} R\left(\frac{a}{M}\right) - \frac{1}{\pi^2} \sum_{a=2}^{\infty} \frac{a^2-1}{a+2} R\left(\frac{a}{M}\right) \\
&= -\frac{3}{4\pi^2} - \frac{2}{\pi^2} \sum_{a=3}^{\infty} \frac{a(a^2-1)}{(a^2-4)} R\left(\frac{a}{M}\right) \\
&= \frac{23}{2\pi^2} - \frac{2}{\pi^2} \sum_{a=1}^{\infty} a R\left(\frac{a}{M}\right) - \frac{6}{\pi^2} \sum_{a=1}^{\infty} \frac{1}{a} R\left(\frac{a}{M}\right) \\
&= -8M^2 C_1 - \frac{6}{\pi^2} \ln\left(\frac{\mathcal{A}_1 M}{\mu}\right) + \frac{35}{3\pi^2} - \frac{6\gamma}{\pi^2}.
\end{aligned} \tag{3.63}$$

Combining all terms so far, we have

$$G_{1-loop} = -24M^2 C_1 + 8M^2 C_2 - \frac{2}{\pi^2} \ln\left(\frac{\mathcal{A}_1 M}{\mu}\right) + \frac{8}{\pi^2} \ln\left(\frac{\mathcal{A}_2 M}{\mu}\right) + \frac{71}{6\pi^2} - \frac{10}{\pi^2} \zeta(3) + \frac{6\gamma}{\pi^2}. \tag{3.64}$$



Figure 3: Counterterm contribution to $\langle A_i A_j \rangle$.

We have in addition the counterterm diagram of figure 3, which receives contributions from the $\text{tr}(A_i A_i)$ and $p^2 \text{tr}(A_i A_i)$ counterterms. These give:

$$G_{ct} = -12Z_0 - 48Z_1 = -12Z_0 - \frac{6}{\pi^2} \ln\left(\frac{M}{\mu}\right) - \frac{16}{5} F_2 - \frac{7}{\pi^2} + \frac{6}{5\pi^2} \ln\left(\frac{\mathcal{A}_1^4}{\mathcal{A}_2^9}\right). \tag{3.65}$$

The final result is

$$G_{cutoff} = G_{1-loop} + G_{ct} = -12Z_0 - 24M^2 C_1 + 8M^2 C_2 - \frac{16}{5} F_2 + \frac{14}{5\pi^2} \ln\left(\frac{\mathcal{A}_1}{\mathcal{A}_2}\right) - \frac{10}{\pi^2} \zeta(3) + \frac{29}{6\pi^2} + \frac{6\gamma}{\pi^2}. \tag{3.66}$$

Demanding that this equals the dimensionally regularized result (3.60) above then determines the coefficient Z_0 to be

$$Z_0 = -\frac{4}{15} F_2 + \frac{7}{30\pi^2} \ln\left(\frac{\mathcal{A}_1}{\mathcal{A}_2}\right) + \frac{5}{18\pi^2} - 2M^2 C_1 + \frac{2}{3} M^2 C_2. \tag{3.67}$$

Thus, the required counterterms for our two-loop calculation are given in (2.13), with the coefficients Z_0 , Z_1 , and Z_2 given in (3.67) and (3.18), respectively.

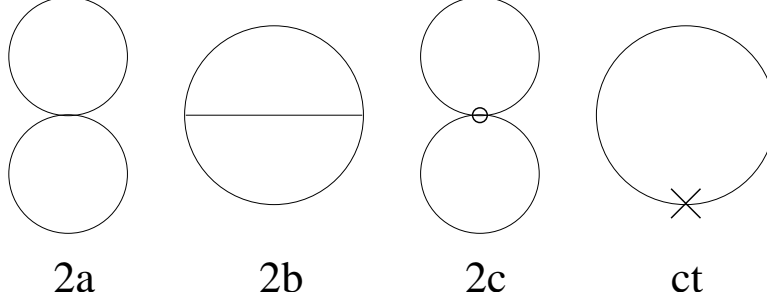


Figure 4: Diagrams that contribute to the 2-loop free energy. The vertex of diagram 2a (2c) corresponds to the first (second) interaction term of (2.10).

4. Evaluating the two-loop diagrams

Now that we have worked out the required counterterms, we are ready to calculate the necessary correlators in (2.20) to determine the partition function. The relevant diagrams are depicted in figure 4. We begin first with the planar contributions.

4.1. Two-loop planar diagrams

From the discussion in section 2.4, the contribution to the partition function from planar diagrams comes from the coefficients of $\text{tr}(U^n)\text{tr}(U^{\dagger n})$ in the expansion in powers of U . We have three two-loop planar diagrams, one from a pair of cubic vertices and one from each of the two quartic vertices. In addition, we have at the same order one-loop planar diagrams for each of the counterterms (2.13).

We begin with the two-loop diagrams, including a regulator function for each A_i line, though we can neglect regulator functions for momenta whose sums are already exponentially suppressed. Full expressions for these diagrams were previously derived in [5]. They are¹⁴ (with summation over the spherical harmonic indices α , β and γ implied)

$$\begin{aligned} S_{2a}^{pl} &= -\beta \frac{g_{YM}^2}{2} (D^{\alpha\beta\gamma} D^{\bar{\alpha}\bar{\beta}\bar{\gamma}} - D^{\alpha\bar{\alpha}\gamma} D^{\beta\bar{\beta}\bar{\gamma}}) \Delta_{j_\alpha}(0, \alpha_{ab}) \Delta_{j_\beta}(0, \alpha_{ac}) \\ &= \frac{2\beta g_{YM}^2}{3\pi^2} j_\alpha(j_\alpha + 2) j_\beta(j_\beta + 2) \Delta_{j_\alpha}(0, \alpha_{ab}) \Delta_{j_\beta}(0, \alpha_{ac}), \end{aligned} \quad (4.1)$$

$$\begin{aligned} S_{2b}^{pl} &= -\frac{\beta g_{YM}^2}{6} \widehat{E}^{\alpha\beta\gamma} \widehat{E}^{\bar{\alpha}\bar{\beta}\bar{\gamma}} \int dt \Delta_{j_\alpha}(t, \alpha_{ab}) \Delta_{j_\beta}(t, \alpha_{bc}) \Delta_{j_\gamma}(t, \alpha_{ca}) \\ &= -\beta g_{YM}^2 \left(\frac{1}{3} (j_\alpha + j_\beta + j_\gamma + 3)^2 R_{4+}^2(j_\alpha, j_\beta, j_\gamma) + (j_\alpha + j_\beta - j_\gamma + 1)^2 R_{4-}^2(j_\alpha, j_\beta, j_\gamma) \right) \\ &\quad \int dt \Delta_{j_\alpha}(t, \alpha_{ab}) \Delta_{j_\beta}(t, \alpha_{bc}) \Delta_{j_\gamma}(t, \alpha_{ca}), \end{aligned} \quad (4.2)$$

¹⁴ Recall that in diagram 2c, we ignore the part proportional to $\delta(0)$.

$$\begin{aligned}
S_{2c}^{pl} &= \beta g_{YM}^2 \frac{D^{\alpha\beta\gamma} D^{\bar{\alpha}\bar{\beta}\bar{\gamma}}}{j_\gamma(j_\gamma + 2)} (D_\tau \Delta_{j_\alpha}(0, \alpha_{ac}) D_\tau \Delta_{j_\beta}(0, \alpha_{ab}) + (j_\beta + 1)^2 \Delta_{j_\alpha}(0, \alpha_{bc}) \Delta_{j_\beta}(0, \alpha_{ab})) \\
&= \frac{2\beta g_{YM}^2}{j_\gamma(j_\gamma + 2)} (R_{3+}^2(j_\alpha, j_\gamma, j_\beta) + R_{3-}^2(j_\alpha, j_\gamma, j_\beta)) \\
&\quad (D_\tau \Delta_{j_\beta}(0, \alpha_{ab}) D_\tau \Delta_{j_\alpha}(0, \alpha_{ac}) + (j_\beta + 1)^2 \Delta_{j_\alpha}(0, \alpha_{bc}) \Delta_{j_\beta}(0, \alpha_{ab})),
\end{aligned} \tag{4.3}$$

where \widehat{E} and the functions $R_{3\pm}$ and $R_{4\pm}$ are defined in appendix B. Here, the first line for each diagram gives the expression for the diagram before performing any sums over angular momenta, while the second line gives the result after summing over everything but total angular momentum quantum numbers (these come into the regulator, which we have not yet written explicitly). Note that for all diagrams, each of the propagators contributes factors of α to two of the three index loops, which we label by a , b , and c . The notation α_{ab} indicates that for the tensor products $(\alpha \otimes 1 - 1 \otimes \alpha)$ appearing in the propagator (2.12), the first and second elements of the tensor product appear in the traces associated with index loops a and b , respectively.

We now expand these expressions in powers of U to read off the required coefficients $f_n(x)$ defined in (2.21), inserting explicit expressions for the regulators at this stage. For all diagrams, we find that

$$f_n(x) = f_1(x^n), \tag{4.4}$$

so we need only give the results for $f_1(x)$.

We find that diagram 2a gives

$$f_1^{2a}(x) = \frac{1}{3\pi^2} (f(x))^2 + \frac{2}{3\pi^2} f(x) \left\{ \sum_{a=1}^{\infty} a R\left(\frac{a}{M}\right) - \sum_{a=1}^{\infty} \frac{1}{a} R\left(\frac{a}{M}\right) \right\}, \tag{4.5}$$

where

$$f(x) \equiv \sum_{b=1}^{\infty} \frac{b(b+2)}{(b+1)} x^{b+1} = \frac{x}{(1-x)^2} + \ln(1-x). \tag{4.6}$$

For diagram 2b, we find

$$\begin{aligned}
f_1^{2b}(x) &= \sum_{a=1}^{\infty} \sum_{b=1}^{\infty} \sum_{c/2=(|a-b|+1)/2}^{(a+b-1)/2} \frac{(b+1)x^{a+c+2} - (a+c+2)x^{b+1}}{2(a+1)(b+1)(c+1)(a+b+c+3)(a+c-b+1)} \\
&\quad \cdot \{ R_{4+}^2(a, b, c)(a+b+c+3)^2 + R_{4-}^2(a, b, c)(a+b-c+1)^2 \\
&\quad + R_{4-}^2(b, c, a)(b+c-a+1)^2 + R_{4-}^2(c, a, b)(c+a-b+1)^2 \} R\left(\frac{a+1}{M}\right) R\left(\frac{c+1}{M}\right).
\end{aligned} \tag{4.7}$$

To see the regulator dependent pieces explicitly, we may expand $R(\frac{c+1}{M})$ about $c = a$ for large a ,

$$R\left(\frac{c+1}{M}\right) = R\left(\frac{a+1}{M}\right) + \frac{c-a}{M}R'\left(\frac{a+1}{M}\right) + \frac{(c-a)^2}{2M^2}R''\left(\frac{a+1}{M}\right) + \dots \quad (4.8)$$

For large a , the sum over c of the summand above with various powers of $(c-a)$ inserted then has the following asymptotic behavior as a function of a :

$$\begin{aligned} \sum &\rightarrow -\frac{1}{3\pi^2}a\frac{b^2-1}{b}x^b - \frac{1}{15\pi^2}\frac{1}{a}\frac{(b^2-1)(8b^2-7)}{b}x^b + \mathcal{O}(1/a^2), \\ \sum(c-a) &\rightarrow -\frac{1}{30\pi^2}\frac{(b^2-1)(b^2-4)}{b}x^b + \mathcal{O}(1/a), \\ \sum(c-a)^2 &\rightarrow -\frac{1}{15\pi^2}a\frac{(b^2-1)(b^2-4)}{b}x^b + \mathcal{O}(1), \end{aligned} \quad (4.9)$$

where we have made the replacements $a \rightarrow a-1$, $b \rightarrow b-1$. The omitted terms lead only to regulator-independent finite contributions. The regulator-dependent terms are then

$$\begin{aligned} f_{2b}^{reg} &= -\frac{1}{3\pi^2}\sum_{b=1}^{\infty}\frac{b^2-1}{b}x^b\sum_{a=1}^{\infty}aR^2\left(\frac{a}{M}\right) \\ &\quad -\frac{1}{15\pi^2}\sum_{b=1}^{\infty}\frac{(b^2-1)(8b^2-7)}{b}x^b\sum_{a=1}^{\infty}\frac{1}{a}R^2\left(\frac{a}{M}\right) \\ &\quad -\frac{1}{M^2}\frac{1}{30\pi^2}\sum_{b=1}^{\infty}\frac{(b^2-1)(b^2-4)}{b}x^b\sum_{a=1}^{\infty}aR\left(\frac{a}{M}\right)R''\left(\frac{a}{M}\right). \end{aligned} \quad (4.10)$$

Note that the term involving $1/M\sum_a R(a/M)R'(a/M)$ is regulator-independent.

For diagram 2c, we find

$$\begin{aligned} f_1^{2c} &= \sum_{a=1}^{\infty}\sum_{b=1}^{\infty}\sum_{c/2=(||a-b|-1|+1)/2}^{(a+b)/2} \frac{1}{c(c+2)}\left\{\frac{b-a}{a+1}x^{a+b+2} + \left(\frac{b+1}{a+1} + \frac{a+1}{b+1}\right)x^{b+1}\right\} \\ &\quad \cdot \{R_{3+}^2(a, c, b) + R_{3-}^2(a, c, b)\}R\left(\frac{a+1}{M}\right). \end{aligned} \quad (4.11)$$

The asymptotic behavior of the sum over c for large a is

$$\sum \rightarrow \frac{1}{3\pi^2}a\frac{b^2-1}{b}x^b + \frac{1}{15\pi^2}\frac{1}{a}\frac{(b^2-1)(8b^2+3)}{b}x^b + \mathcal{O}(1/a^2). \quad (4.12)$$

The regulator-dependent terms are then

$$\begin{aligned} f_{2c}^{reg} &= \frac{1}{3\pi^2}\sum_{b=1}^{\infty}\frac{b^2-1}{b}x^b\sum_{a=1}^{\infty}aR\left(\frac{a}{M}\right) \\ &\quad + \frac{1}{15\pi^2}\sum_{b=1}^{\infty}\frac{(b^2-1)(8b^2+3)}{b}x^b\sum_{a=1}^{\infty}\frac{1}{a}R\left(\frac{a}{M}\right). \end{aligned} \quad (4.13)$$

Combining all the regulator-dependent terms and carefully comparing the divergent sums to the divergent integrals defined in (3.14), we find

$$f^{reg} = f(x)\left(4C_1M^2 - \frac{4}{3}C_2M^2 - \frac{1}{18\pi^2}\right) + \frac{1}{15\pi^2}(8g(x) - 7f(x))\ln\left(\frac{\mathcal{A}_1}{\mathcal{A}_2}\right) + \frac{2}{15}F_2(4f(x) - g(x)), \quad (4.14)$$

where $f(x)$ is as above, and

$$g(x) \equiv \sum_{b=1}^{\infty} b(b^2 - 1)x^b = \frac{6x^2}{(1-x)^4}. \quad (4.15)$$

The expression (4.14) will be useful in verifying that all regulator dependence cancels, though in practice, we simply need to use (4.5), (4.7), and (4.11) with any convenient choice of regulator.

4.2. Counterterms

To the expressions above, we must add the counterterm contributions, coming from the single-trace counterterms in (2.13). Using this expression, we find

$$S_{eff}^{ct} = \langle S_{ct} \rangle = \beta g_{YM}^2 N \sum_{\alpha} (Z_0 + (Z_1 - Z_2)(j_{\alpha} + 1)^2) \Delta_{j_{\alpha}}(0, \alpha_{ab}). \quad (4.16)$$

To determine the term proportional to Z_2 , we have used the fact that

$$(-D_{\tau}^2 + (j+1)^2)\Delta_j(t, \alpha) = \delta(t), \quad (4.17)$$

ignoring the resulting $\delta(0)$ term, which will be cancelled by another diagram which is independent of U and the temperature.

Expanding this to find the coefficient of $\text{tr}(U^n)\text{tr}(U^{\dagger n})$ and performing the angular momentum sum, we find that the counterterm contribution to f_n is $f_n^{ct}(x) = f_1^{ct}(x^n)$, where

$$f_1^{ct}(x) = 2Z_0f(x) + 2(Z_1 - Z_2)g(x). \quad (4.18)$$

Using the expressions (3.18) and (3.67) above, this becomes

$$f_1^{ct}(x) = f(x) \left[M^2\left(-4C_1 + \frac{4}{3}C_2\right) + \frac{7}{15\pi^2} \ln\left(\frac{\mathcal{A}_1}{\mathcal{A}_2}\right) - \frac{8}{15}F_2 + \frac{5}{9\pi^2} \right] \\ + g(x) \left[\frac{2}{15}F_2 + \frac{1}{4\pi^2} - \frac{8}{15\pi^2} \ln\left(\frac{\mathcal{A}_1}{\mathcal{A}_2}\right) \right]. \quad (4.19)$$

Comparing this with the regulator-dependent pieces (4.14) above, we see that all regulator dependence cancels in the sum $f_1^{2a} + f_1^{2b} + f_1^{2c} + f_1^{ct}$. Thus, our final result is

$$f_n(x) = f_1(x^n), \quad (4.20)$$

where $f_1(x)$ is the sum of (4.19), (4.5), (4.7), and (4.11), which is finite and regulator independent. This may be computed numerically for any value of x , and we do indeed find that the numerical results are independent of the regulator used. The perturbative expansion of f_1 at small x takes the form

$$f_1(x) = \frac{1}{4\pi^2}x^2 + \frac{4}{\pi^2}x^3 + \frac{55}{4\pi^2}x^4 + \dots, \quad (4.21)$$

and its value at the critical temperature (1.2) is given by

$$f_1(x_{c,0}) \simeq 0.0253. \quad (4.22)$$

The functions $f_n(x)$ determine the planar contribution to the two-loop partition function via (2.23) while $f_1(x)$ determines the perturbative shift in the Hagedorn temperature, which we compute using (2.26) in section 4.5 below.

4.3. Two-loop non-planar diagrams

We now turn to the non-planar contribution to the two-loop partition function. In this case, since there is only a single index loop, and since each term in the propagators contributes an equal number of U 's and U^\dagger 's, we will always end up with just the identity matrix inside the single trace. Equivalently, we can simply set $\alpha = 0$ ($U = 1$) in all propagators from the start. The resulting temperature-dependent but U -independent expressions contribute directly to the two-loop free energy via (2.24).

We find that the expressions for the three non-planar diagrams are related to the expressions (4.1)-(4.3) for the planar diagrams by setting $\alpha = 0$ and including an overall factor of $-1/N^2$.¹⁵ Thus, we have

$$\begin{aligned} S_{2a}^{np} &= \beta \frac{g_{YM}^2}{2} (D^{\alpha\beta\gamma} D^{\bar{\alpha}\bar{\beta}\bar{\gamma}} - D^{\alpha\bar{\alpha}\gamma} D^{\beta\bar{\beta}\bar{\gamma}}) \Delta_{j_\alpha}(0,0) \Delta_{j_\beta}(0,0) \\ &= -\frac{2\beta g_{YM}^2}{3\pi^2} j_\alpha(j_\alpha + 2) j_\beta(j_\beta + 2) \Delta_{j_\alpha}(0,0) \Delta_{j_\beta}(0,0), \end{aligned} \quad (4.23)$$

¹⁵ This is related to the fact that the planar and non-planar diagrams must cancel for the Abelian theory with $N = 1$, which is free.

$$\begin{aligned}
S_{2b}^{np} &= \frac{\beta g_{YM}^2}{6} \widehat{E}^{\alpha\beta\gamma} \widehat{E}^{\bar{\alpha}\bar{\beta}\bar{\gamma}} \int dt \Delta_{j_\alpha}(t, 0) \Delta_{j_\beta}(t, 0) \Delta_{j_\gamma}(t, 0) \\
&= \beta g_{YM}^2 \left(\frac{1}{3} (j_\alpha + j_\beta + j_\gamma + 3)^2 R_{4+}^2(j_\alpha, j_\beta, j_\gamma) + (j_\alpha + j_\beta - j_\gamma + 1)^2 R_{4-}^2(j_\alpha, j_\beta, j_\gamma) \right) \\
&\quad \int dt \Delta_{j_\alpha}(t, 0) \Delta_{j_\beta}(t, 0) \Delta_{j_\gamma}(t, 0),
\end{aligned} \tag{4.24}$$

$$\begin{aligned}
S_{2c}^{np} &= -\beta g_{YM}^2 \frac{D^{\alpha\beta\gamma} D^{\bar{\alpha}\bar{\beta}\bar{\gamma}}}{j_\gamma(j_\gamma + 2)} (D_\tau \Delta_{j_\alpha}(0, 0) D_\tau \Delta_{j_\beta}(0, 0) + (j_\beta + 1)^2 \Delta_{j_\alpha}(0, 0) \Delta_{j_\beta}(0, 0)) \\
&= -\frac{2\beta g_{YM}^2}{j_\gamma(j_\gamma + 2)} (R_{3+}^2(j_\alpha, j_\gamma, j_\beta) + R_{3-}^2(j_\alpha, j_\gamma, j_\beta)) \\
&\quad (D_\tau \Delta_{j_\beta}(0, 0) D_\tau \Delta_{j_\alpha}(0, 0) + (j_\beta + 1)^2 \Delta_{j_\alpha}(0, 0) \Delta_{j_\beta}(0, 0)).
\end{aligned} \tag{4.25}$$

In each case, the group indices are contracted into a single (trivial) trace which gives an overall factor of N . We will find again that the angular momentum sums here are divergent, but there are additional counterterms coming from the double-trace terms in (2.13). The result for these is obtained from the result for the single-trace counterterms in the same way that the non-planar two-loop contributions are obtained from the planar two-loop contributions.

Using this relation between planar diagrams/single-trace counterterms and non-planar diagrams/double-trace counterterms, it follows from (2.21) that the full contribution to $S_{2\text{-loop}}^{\text{eff}}$ may be written as

$$\begin{aligned}
S_{pl+np}^{\text{eff}} &= \beta g_{YM}^2 N \sum_{n=1}^{\infty} f_n(x) (\text{tr}(U^n) \text{tr}(U^{\dagger n}) - 1) \\
&\quad + \beta g_{YM}^2 \sum_{n \geq m > 0} f_{nm}(x) \{ \text{tr}(U^n) \text{tr}(U^m) \text{tr}(U^{-n-m}) + c.c. - 2N \}.
\end{aligned} \tag{4.26}$$

For the planar diagrams, the two-trace terms in the first line arose from the combination of divergent two-loop contributions plus counterterms to yield the finite regulator-independent results defined by $f_n(x) = f_1(x^n)$. While we did not calculate the three trace terms explicitly, it is straightforward to show that they are manifestly finite. It immediately follows that all divergences and regulator-dependence cancel also for the non-planar diagrams plus double-trace counterterms.

Focusing back on the non-planar terms that we need to calculate, it is convenient to use (4.26) to write

$$F_2^{np}(x) = - \sum_{n=1}^{\infty} f_1(x^n) + \widetilde{F}^{np}(x), \tag{4.27}$$

since we have already computed $f_1(x)$; it remains only to calculate

$$\tilde{F}_2^{np}(x) = -2 \sum_{n \geq m > 0} f_{nm}(x), \quad (4.28)$$

where $f_{nm}(x)$ may be computed from the expressions (4.1)-(4.3). Diagram by diagram, we find

$$\begin{aligned} \tilde{F}_{2a}^{np} &= - \sum_{j_\alpha=0}^{\infty} \sum_{j_\beta=0}^{\infty} \frac{1}{6\pi^2} \frac{j_\alpha(j_\alpha+2)j_\beta(j_\beta+2)}{(j_\alpha+1)(j_\beta+1)} \\ &\quad \left(\frac{(1+x^{j_\alpha+1})(1+x^{j_\beta+1})}{(1-x^{j_\alpha+1})(1-x^{j_\beta+1})} - \frac{(1+x^{j_\beta+1})}{(1-x^{j_\beta+1})} - \frac{(1+x^{j_\alpha+1})}{(1-x^{j_\alpha+1})} - 2 \frac{x^{j_\alpha+j_\beta+2}}{1-x^{j_\alpha+j_\beta+2}} + 1 \right), \quad (4.29) \\ \tilde{F}_{2b}^{np} &= \sum_{j_\alpha=1}^{\infty} \sum_{j_\beta=1}^{\infty} \sum_{j_\gamma/2=(|j_\alpha-j_\beta|+1)/2}^{(j_\alpha+j_\beta-1)/2} \\ &\quad \frac{(R_{4+}^2(j_\alpha, j_\beta, j_\gamma)(j_\alpha+j_\beta+j_\gamma+3)^2 + 3R_{4-}^2(j_\alpha, j_\beta, j_\gamma)(j_\alpha+j_\beta-j_\gamma+1)^2)}{12(j_\alpha+1)(j_\beta+1)(j_\gamma+1)} \\ &\quad \left[\frac{1}{j_\alpha+j_\beta+j_\gamma+3} - \frac{1}{(1-x^{j_\alpha+1})(1-x^{j_\beta+1})(1-x^{j_\gamma+1})} \right. \\ &\quad \left. \left\{ \frac{1-x^{j_\alpha+j_\beta+j_\gamma+3}}{j_\alpha+j_\beta+j_\gamma+3} + \frac{x^{j_\alpha+1}-x^{j_\beta+j_\gamma+2}}{j_\beta+j_\gamma-j_\alpha+1} + \frac{x^{j_\beta+1}-x^{j_\alpha+j_\gamma+2}}{j_\alpha+j_\gamma-j_\beta+1} + \frac{x^{j_\gamma+1}-x^{j_\alpha+j_\beta+2}}{j_\alpha+j_\beta-j_\gamma+1} \right\} \right. \\ &\quad + \frac{2}{(j_\alpha+j_\beta+j_\gamma+3)(j_\alpha+j_\beta-j_\gamma+1)} \left\{ \frac{(j_\alpha+j_\beta+1)x^{j_\gamma+1}}{1-x^{j_\gamma+1}} - \frac{(j_\gamma+1)x^{j_\alpha+j_\beta+2}}{1-x^{j_\alpha+j_\beta+2}} \right\} \\ &\quad + \frac{2}{(j_\alpha+j_\beta+j_\gamma+3)(j_\beta+j_\gamma-j_\alpha+1)} \left\{ \frac{(j_\beta+j_\gamma+1)x^{j_\alpha+1}}{1-x^{j_\alpha+1}} - \frac{(j_\alpha+1)x^{j_\beta+j_\gamma+2}}{1-x^{j_\beta+j_\gamma+2}} \right\} \\ &\quad \left. + \frac{2}{(j_\alpha+j_\beta+j_\gamma+3)(j_\gamma+j_\alpha-j_\beta+1)} \left\{ \frac{(j_\gamma+j_\alpha+1)x^{j_\beta+1}}{1-x^{j_\beta+1}} - \frac{(j_\beta+1)x^{j_\gamma+j_\alpha+2}}{1-x^{j_\gamma+j_\alpha+2}} \right\} \right], \quad (4.30) \end{aligned}$$

and

$$\begin{aligned} \tilde{F}_{2c}^{np} &= \sum_{j_\alpha=1}^{\infty} \sum_{j_\beta=1}^{\infty} \sum_{j_\gamma/2=(|j_\alpha-j_\beta|-1|+1)/2}^{(j_\alpha+j_\beta)/2} \frac{1}{j_\gamma(j_\gamma+2)} (R_{3+}^2(j_\alpha, j_\gamma, j_\beta) + R_{3-}^2(j_\alpha, j_\gamma, j_\beta)) \\ &\quad \left\{ \frac{j_\beta+1}{j_\alpha+1} \left(\frac{(1+x^{j_\alpha+1})(1+x^{j_\beta+1})}{(1-x^{j_\alpha+1})(1-x^{j_\beta+1})} - \frac{(1+x^{j_\beta+1})}{(1-x^{j_\beta+1})} - \frac{(1+x^{j_\alpha+1})}{(1-x^{j_\alpha+1})} \right) \right. \\ &\quad \left. - \left(\frac{j_\beta+1}{j_\alpha+1} - 1 \right) \frac{2x^{j_\alpha+j_\beta+2}}{(1-x^{j_\alpha+j_\beta+2})} \right\}. \quad (4.31) \end{aligned}$$

Using (4.27), these results, combined with our results for $f_1(x)$ in section 4.2, give the final result for F_2^{np} , which in turn gives the non-planar contribution to the two-loop partition function and free energy via (2.23) and (2.24).

4.4. Results: Two-loop partition function

We have now calculated all the elements necessary to give the full two-loop partition function. Using (2.23) and (4.27), we find that the two-loop partition function for $U(N)$ Yang-Mills theory at large N on a small S^3 is

$$Z_{2-loop}^{U(N)} = e^{-\lambda\beta\tilde{F}_2^{np}(x)} \prod_{n=1}^{\infty} \frac{e^{\lambda\beta f_1(x^n)}}{1 - z(x^n) + \lambda n\beta f_1(x^n)} + \mathcal{O}(\lambda^2), \quad (4.32)$$

where $z(x)$ is given in (2.16), $\tilde{F}_2^{np}(x)$ is the sum of (4.29), (4.30), and (4.31), and $f_1(x)$ is the sum of (4.5), (4.7), (4.11), and (4.19). To get the $SU(N)$ result, we simply divide by $Z_{U(1)}$, yielding

$$Z_{2-loop}^{SU(N)} = e^{-\lambda\beta\tilde{F}_2^{np}(x)} \prod_{n=1}^{\infty} \frac{e^{-z(x^n)/n + \lambda\beta f_1(x^n)}}{1 - z(x^n) + \lambda n\beta f_1(x^n)} + \mathcal{O}(\lambda^2). \quad (4.33)$$

For either $U(N)$ or $SU(N)$, the order λ correction to the free energy (using (2.24)) is

$$\delta F = -T\delta \ln(Z) = \lambda \left[\tilde{F}_2^{np}(x) + \sum_{n=1}^{\infty} f_1(x^n) \left(\frac{n}{1 - z(x^n)} - 1 \right) \right]. \quad (4.34)$$

Our results for the two-loop partition function can be expanded in powers of x as in (1.1), from which we can read off the sum of energy corrections for all states with a given energy in the free theory, since

$$\sum_i x^{E_0 + \lambda\delta E_i} = x^{E_0} \left(1 + \lambda \ln(x) \sum_i \delta E_i + \mathcal{O}(\lambda^2) \right). \quad (4.35)$$

For $SU(N)$, we find that the first few terms in the series give

$$Z_{2-loop}^{SU(N)} = 1 + \left(21 + \frac{4}{\pi^2} \lambda \ln(x) \right) x^4 + \left(96 + \frac{28}{\pi^2} \lambda \ln(x) \right) x^5 + \left(392 + \frac{178}{\pi^2} \lambda \ln(x) \right) x^6 + \dots \quad (4.36)$$

Thus, for example, the sum of perturbative energy shifts for the 21 independent states with energy $4/R_{S^3}$ is $4\lambda/\pi^2$.

Since the free Yang-Mills theory in the small volume limit is conformal, we have a map between states in this theory and local operators in Euclidean Yang-Mills theory on \mathbb{R}^4 . The coefficient of the term proportional to $x^n \ln(x)$ is then interpreted as the sum of anomalous dimensions for all operators with dimension n . Thus, we can use the results of [2] for anomalous dimensions of operators in pure Yang-Mills theory as a check on our results (see section 5.1 below).

4.5. Results: Order λ correction to critical temperature

As explained in section 2.4, the two-loop corrections to the partition function will shift the critical temperature associated with the Hagedorn and deconfinement transitions. To compute the shift in x_c or T_c , we use (2.26) or (2.27), which only involve the result (4.22) for $f_1(x_c)$. Recalling from section 2.3 that $x_{c,0} = 2 - \sqrt{3}$ for $\lambda = 0$, we find

$$\delta x_c = 0.00298\lambda, \quad (4.37)$$

so the transition occurs at

$$x_c = 2 - \sqrt{3} + 0.00298\lambda + \mathcal{O}(\lambda^2). \quad (4.38)$$

Equivalently, from (2.27), the critical temperature to order λ is

$$T_c R_{S^3} = T_{c,0} R_{S^3} \cdot \left(1 + \frac{0.00298\lambda}{(2 - \sqrt{3}) \ln(2 + \sqrt{3})} + \mathcal{O}(\lambda^2) \right). \quad (4.39)$$

Below, we will reproduce this result using a formula in [6] for the shift in the transition temperature from anomalous dimensions, providing a strong quantitative check of our results.

5. Checks

5.1. Anomalous dimensions for low-dimension operators

As a first check on our results, we will try to reproduce our result (4.36) for the leading terms in the expansion of the $SU(N)$ partition function using the results of [2] for anomalous dimensions of operators in pure Yang-Mills theory.

Explicit results for the one-loop anomalous dimensions for low-dimension operators in pure large N $SU(N)$ Yang-Mills theory are given in table 1 of [2]. They show that two of the dimension four states have anomalous dimension $-(11/3)(\lambda/8\pi^2)$, ten have anomalous dimension $(7/3)(\lambda/8\pi^2)$, and nine have vanishing anomalous dimension, while at dimension five the 16 primary states have anomalous dimension $3(\lambda/8\pi^2)$ (and each of the dimension four primary states that has an anomalous dimension has four descendants). Adding also all the dimension six states, we find that the results of [2] lead to

$$Z_{2-loop}(x) = 1 + \left(21 + \frac{2\lambda}{\pi^2} \ln(x) \right) x^4 + \left(96 + \frac{14\lambda}{\pi^2} \ln(x) \right) x^5 + \left(392 + \frac{89\lambda}{\pi^2} \ln(x) \right) x^6 + \dots \quad (5.1)$$

This precisely agrees with our result (4.36), if we recall that, due to a difference in conventions, λ in [2] is twice the λ that we used in our computation (as was also the case for the comparison of the flat-space two-loop partition functions in [5]).

5.2. Shift in T_c from anomalous dimensions

In this section, we use an alternate method, based on [6], to check our result for the order λ shift in the transition temperature.

Single trace operators in pure Yang-Mills theory may be put in one to one correspondence with spin chains of lengths $l = 1, 2, \dots, \infty$, where the spins in these chains are vectors in one of two representations of the conformal group. The primaries of these representations are the self-dual and anti-self-dual parts of $F_{\mu\nu}$ and carry quantum numbers $(1, 0, 2)$ and $(0, 1, 2)$, respectively, under (j_1, j_2, Δ) (j_1 labels the representation of the first $SU(2)$, j_2 of the second $SU(2)$, and Δ is the scaling dimension). We will call these two representations chiral c and anti-chiral \bar{c} , respectively. It was demonstrated in [2] that

$$c \times c = (0, 0, 4) + (1, 0, 4) + (2, 0, 4) + \sum_{j=1}^{\infty} (2 + \frac{j}{2}, \frac{j}{2}, 4 + j). \quad (5.2)$$

The tensor product of \bar{c} with \bar{c} is obtained from (5.2) by a $j_1 \leftrightarrow j_2$ flip. Finally,

$$c \times \bar{c} = \sum_{j=2}^{\infty} (\frac{j}{2}, \frac{j}{2}, 2 + j). \quad (5.3)$$

We now list $\chi_R = \text{Tr}_R(x^\Delta)$, the characters for all these representations (they will be needed below). Actually, we will find it more convenient to list $\chi'_R \equiv (1-x)^4 \chi_R$:

$$\begin{aligned} \chi'_{0,0,4} &= x^4, & \chi'_{0,1,4} &= 3x^4, & \chi'_{0,2,4} &= 5x^4, \\ \chi'_{2+\frac{j}{2}, \frac{j}{2}, 4+j} &= (5+j)(j+1)x^{4+j} - j(4+j)x^{5+j}, \\ \chi'_{\frac{j}{2}, \frac{j}{2}, 2+j} &= (j+1)^2 x^{j+2} - j^2 x^{j+3}. \end{aligned} \quad (5.4)$$

According to equation (6.10) of [6],

$$\frac{\delta x_c}{x_{c,0}} = -\frac{\lambda \ln(x_{c,0})}{4\pi^2 x_{c,0} z'(x_{c,0})} \times \langle D_2(x_{c,0}) \rangle, \quad (5.5)$$

where $z(x)$ was defined in (2.16), $\langle D_2(x) \rangle$ is (see equations (4.4) and (4.8) in [2])¹⁶

$$\begin{aligned} \langle D_2(x) \rangle &= -\frac{11}{3} \chi_{0,0,4} + \frac{1}{3} \chi_{0,1,4} + \frac{7}{3} \chi_{0,2,4} + \sum_{j=1}^{\infty} \left(4h(j+2) - \frac{11}{3} \right) \chi_{2+\frac{j}{2}, \frac{j}{2}, 4+j} \\ &\quad + \sum_{j=2}^{\infty} 2(h(j-2) + h(j+2) - 11/6) \chi_{\frac{j}{2}, \frac{j}{2}, 2+j}, \end{aligned} \quad (5.6)$$

¹⁶ Note that here, unlike the previous subsection, we are using the same conventions for λ as in the rest of the paper.

and $h(j) \equiv \sum_{k=1}^j 1/k$ (with $h(0) = 0$).

It is easy to numerically evaluate the sum (5.6) at the Hagedorn temperature, or to compute it analytically using

$$\langle D_2(x) \rangle = \frac{1}{(1-x)^6} \left[2(-\ln(1-x))(1-3x-3x^2+x^3)^2 - 2x + 11x^2 - \frac{2}{3}x^3 - 26x^4 + 36x^5 - \frac{23}{3}x^6 \right]. \quad (5.7)$$

Using (5.5), we find

$$\langle D_2(x_{c,0}) \rangle = (28 - 16\sqrt{3}) / (\sqrt{3} - 1)^4 = 1 \rightarrow \delta T_c / T_{c,0} = \frac{\lambda}{12\pi^2} \langle D_2(x_{c,0}) \rangle = \frac{\lambda}{12\pi^2}, \quad (5.8)$$

or

$$\begin{aligned} T_c R_{S^3} &= T_{c,0} R_{S^3} \cdot \left(1 + \frac{\lambda}{12\pi^2} + \mathcal{O}(\lambda^2) \right) \\ &= T_{c,0} R_{S^3} \cdot \left(1 + \frac{1}{(2-\sqrt{3}) \ln(2+\sqrt{3})} \left[\frac{(2-\sqrt{3}) \ln(2+\sqrt{3}) \lambda}{12\pi^2} \right] + \mathcal{O}(\lambda^2) \right). \end{aligned} \quad (5.9)$$

Finally, given

$$\frac{(2-\sqrt{3}) \ln(2+\sqrt{3})}{12\pi^2} \approx 0.00298, \quad (5.10)$$

we find perfect agreement with (4.39) (within our numerical accuracy). Note that, in general, in order to have agreement between (2.26) and (5.5), we should have

$$f_1(x_{c,0}) = \frac{\langle D_2(x_{c,0}) \rangle}{4\pi^2}, \quad (5.11)$$

which is indeed obeyed (within our accuracy) by our result (4.22).

Acknowledgements

We would like to thank Shiraz Minwalla and Kyriakos Papadodimas for helpful discussions and collaboration during the early part of this work. OA would like to thank Harvard University, the Aspen Center for Physics and the Institute for Advanced Study for hospitality during the course of this work. MVR would like to thank the Weizmann Institute of Science for hospitality while part of this work was completed. The work of OA was supported in part by the Israel-U.S. Binational Science Foundation, by the Israel Science Foundation (grant number 1399/04), by the Braun-Roger-Siegl foundation, by the European network HPRN-CT-2000-00122, by a grant from the G.I.F., the German-Israeli Foundation for Scientific Research and Development, by Minerva, by a grant of DIP (H.52), and by the Schrum foundation. The work of JM was supported in part by an NSF Graduate Research Fellowship and by DOE grant DE-FG01-91ER40654. The work of MVR was supported in part by the Natural Sciences and Engineering Council of Canada, by the Canada Research Chairs programme, and by the Alfred P. Sloan Foundation.

Appendix A. Actions and propagators

The quadratic action for gauge-fixed Euclidean pure Yang-Mills theory on $S^3 \times S^1$, as described in §2, is given by (with $D_\tau \equiv \partial_t - i[\alpha, \cdot]$)

$$S_2 = \int dt \operatorname{tr} \left(\frac{1}{2} A^{\bar{\alpha}} (-D_\tau^2 + (j_\alpha + 1)^2) A^\alpha + \frac{1}{2} a^{\bar{\alpha}} j_\alpha (j_\alpha + 2) a^\alpha + \bar{c}^{\bar{\alpha}} j_\alpha (j_\alpha + 2) c^\alpha \right). \quad (\text{A.1})$$

In addition, we have cubic interactions

$$S_3 = g_{YM} \int dt \operatorname{tr} \left(i \bar{c}^{\bar{\alpha}} [A^\gamma, c^\beta] C^{\bar{\alpha}\gamma\beta} + 2i a^\alpha A^\gamma a^\beta C^{\alpha\gamma\beta} - i [A^\alpha, D_\tau A^\beta] a^\gamma D^{\alpha\beta\gamma} + i A^\alpha A^\beta A^\gamma \epsilon_\alpha (j_\alpha + 1) E^{\alpha\beta\gamma} \right), \quad (\text{A.2})$$

and quartic interactions

$$S_4 = g_{YM}^2 \int dt \operatorname{tr} \left(-\frac{1}{2} [a^\alpha, A^\beta] [a^\gamma, A^\delta] \left(D^{\beta\bar{\lambda}\alpha} D^{\delta\lambda\gamma} + \frac{1}{j_\lambda (j_\lambda + 2)} C^{\alpha\beta\bar{\lambda}} C^{\gamma\delta\lambda} \right) - \frac{1}{2} A^\alpha A^\beta A^\gamma A^\delta \left(D^{\alpha\gamma\bar{\lambda}} D^{\beta\delta\lambda} - D^{\alpha\delta\bar{\lambda}} D^{\beta\gamma\lambda} \right) \right). \quad (\text{A.3})$$

The quantities C , D , and E are integrals over spherical harmonics, and are defined in appendix B. The propagators of the various fields follow from (A.1) and are given by

$$\langle \bar{c}_{ab}^{\bar{\alpha}}(t) c_{cd}^\beta(t') \rangle = \frac{1}{j_\alpha (j_\alpha + 2)} \delta^{\alpha\beta} \delta(t - t') \delta_{ad} \delta_{cb}, \quad (\text{A.4})$$

$$\langle a_{ab}^\alpha(t) a_{cd}^\beta(t') \rangle = \frac{1}{j_\alpha (j_\alpha + 2)} \delta^{\alpha\beta} \delta(t - t') \delta_{ad} \delta_{cb}, \quad (\text{A.5})$$

$$\langle A_{ab}^\alpha(t) A_{cd}^\beta(t') \rangle = \delta^{\alpha\beta} \Delta_{j_\alpha}^{ad,cb}(t - t', \alpha), \quad (\text{A.6})$$

where Δ is defined in section 2.

Appendix B. Spherical harmonics on S^3

A detailed discussion of spherical harmonics on S^3 may be found in appendix B of [5]. Here, we collect various formulae relevant for the present calculation. Many of the basic results were derived in [12].

B.1. Basic properties of spherical harmonics

Scalar functions on the sphere may be expanded in a complete set of spherical harmonics $S_j^{m m'}$ transforming in the $(j/2, j/2)$ representation of $SU(2) \times SU(2) \equiv SO(4)$, where j is any non-negative integer, and $-j/2 \leq m, m' \leq j/2$. It is convenient to denote the full set of indices (j, m, m') by α . These obey an orthonormality condition (we take the radius of the S^3 to be one)

$$\int_{S^3} S^\alpha S^{\bar{\beta}} = \delta^{\alpha\bar{\beta}}, \quad (\text{B.1})$$

where $S^{\bar{\alpha}}$ denotes the complex conjugate of S^α ,

$$(S_j^{m m'})^* = (-1)^{m+m'} S_j^{-m -m'}. \quad (\text{B.2})$$

The spherical harmonics are eigenfunctions of the Laplace operator on the sphere,

$$\nabla^2 S^\alpha = -j_\alpha(j_\alpha + 2)S^\alpha, \quad (\text{B.3})$$

and under a parity operation transform with eigenvalue $(-1)^{j_\alpha}$.

A general vector field on the sphere may be expanded as a combination of gradients of the scalar spherical harmonics plus a set of vector spherical harmonics $\vec{V}_{j\pm}^{m m'}$. These transform in the $(\frac{j\pm 1}{2}, \frac{j\mp 1}{2})$ representation of $SO(4)$, where j is a positive integer. Again, it is convenient to denote the full set of indices (j, m, m', ϵ) by a single index α . These obey orthonormality relations

$$\begin{aligned} \int_{S^3} \vec{V}^\alpha \cdot \vec{V}^\beta &= \delta^{\alpha\bar{\beta}}, \\ \int_{S^3} \vec{V}^\alpha \cdot \vec{\nabla} S^\beta &= 0. \end{aligned} \quad (\text{B.4})$$

Again $V^{\bar{\alpha}}$ indicates the complex conjugate of V^α , given by

$$(\vec{V}_{j\pm}^{m m'})^* = (-1)^{m+m'+1} \vec{V}_{j\pm}^{-m -m'}. \quad (\text{B.5})$$

The vector spherical harmonics are eigenfunctions of parity with eigenvalue $(-1)^{j+1}$, and satisfy

$$\begin{aligned} \nabla^2 \vec{V}^\alpha &= -(j_\alpha + 1)^2 \vec{V}^\alpha, \\ \vec{\nabla} \times \vec{V}^\alpha &= -\epsilon_\alpha(j_\alpha + 1) \vec{V}^\alpha, \\ \vec{\nabla} \cdot \vec{V}^\alpha &= 0. \end{aligned} \quad (\text{B.6})$$

Explicit expressions for the scalar and vector spherical harmonics may be found in [12].

B.2. Spherical harmonic integrals

The vertices of the mode-expanded Yang-Mills theory on S^3 have coefficients involving integrals over three spherical harmonics. We define

$$\begin{aligned}
B^{\alpha\beta\gamma} &\equiv \int_{S^3} S^\alpha S^\beta S^\gamma, \\
C^{\alpha\beta\gamma} &\equiv \int_{S^3} S^\alpha \vec{V}^\beta \cdot \vec{\nabla} S^\gamma, \\
D^{\alpha\beta\gamma} &\equiv \int_{S^3} \vec{V}^\alpha \cdot \vec{V}^\beta S^\gamma, \\
E^{\alpha\beta\gamma} &\equiv \int_{S^3} \vec{V}^\alpha \cdot (\vec{V}^\beta \times \vec{V}^\gamma).
\end{aligned} \tag{B.7}$$

It is also convenient to define

$$\begin{aligned}
\widehat{B}^{\alpha\beta\gamma} &\equiv \frac{1}{j_\alpha(j_\alpha + 2)j_\beta(j_\beta + 2)} \int_{S^3} (\vec{\nabla} S^\alpha) \cdot (\vec{\nabla} S^\beta) S^\gamma \\
&= \frac{1}{2} \frac{(j_\alpha(j_\alpha + 2) + j_\beta(j_\beta + 2) - j_\gamma(j_\gamma + 2))}{j_\alpha(j_\alpha + 2)j_\beta(j_\beta + 2)} B^{\alpha\beta\gamma}, \\
\widehat{E}^{\alpha\beta\gamma} &\equiv E^{\alpha\beta\gamma} (\epsilon_\alpha(j_\alpha + 1) + \epsilon_\beta(j_\beta + 1) + \epsilon_\gamma(j_\gamma + 1)).
\end{aligned} \tag{B.8}$$

These integrals were calculated in [12], and the results may be expressed as¹⁷

$$\begin{aligned}
B^{\alpha\beta\gamma} &= \begin{pmatrix} \frac{j_\alpha}{2} & \frac{j_\beta}{2} & \frac{j_\gamma}{2} \\ m_\alpha & m_\beta & m_\gamma \end{pmatrix} \begin{pmatrix} \frac{j_\alpha}{2} & \frac{j_\beta}{2} & \frac{j_\gamma}{2} \\ m'_\alpha & m'_\beta & m'_\gamma \end{pmatrix} R_1(j_\alpha, j_\beta, j_\gamma), \\
C^{\alpha\beta\gamma} &= \begin{pmatrix} \frac{j_\alpha}{2} & \frac{j_\beta + \epsilon_\beta}{2} & \frac{j_\gamma}{2} \\ m_\alpha & m_\beta & m_\gamma \end{pmatrix} \begin{pmatrix} \frac{j_\alpha}{2} & \frac{j_\beta - \epsilon_\beta}{2} & \frac{j_\gamma}{2} \\ m'_\alpha & m'_\beta & m'_\gamma \end{pmatrix} R_2(j_\alpha, j_\beta, j_\gamma), \\
D^{\alpha\beta\gamma} &= \begin{pmatrix} \frac{j_\alpha + \epsilon_\alpha}{2} & \frac{j_\beta + \epsilon_\beta}{2} & \frac{j_\gamma}{2} \\ m_\alpha & m_\beta & m_\gamma \end{pmatrix} \begin{pmatrix} \frac{j_\alpha - \epsilon_\alpha}{2} & \frac{j_\beta - \epsilon_\beta}{2} & \frac{j_\gamma}{2} \\ m'_\alpha & m'_\beta & m'_\gamma \end{pmatrix} R_{3\epsilon_\alpha\epsilon_\beta}(j_\alpha, j_\beta, j_\gamma), \\
E^{\alpha\beta\gamma} &= \begin{pmatrix} \frac{j_\alpha + \epsilon_\alpha}{2} & \frac{j_\beta + \epsilon_\beta}{2} & \frac{j_\gamma + \epsilon_\gamma}{2} \\ m_\alpha & m_\beta & m_\gamma \end{pmatrix} \begin{pmatrix} \frac{j_\alpha - \epsilon_\alpha}{2} & \frac{j_\beta - \epsilon_\beta}{2} & \frac{j_\gamma - \epsilon_\gamma}{2} \\ m'_\alpha & m'_\beta & m'_\gamma \end{pmatrix} R_{4\epsilon_\alpha\epsilon_\beta\epsilon_\gamma}(j_\alpha, j_\beta, j_\gamma),
\end{aligned} \tag{B.9}$$

where

$$R_1(x, y, z) = \frac{(-1)^\sigma}{\pi} \left(\frac{(x+1)(y+1)(z+1)}{2} \right)^{\frac{1}{2}}, \tag{B.10}$$

$$R_2(x, y, z) = \frac{(-1)^{\sigma'}}{\pi} \left[\frac{(x+1)(z+1)(\sigma' - x)(\sigma' - y)(\sigma' - z)(\sigma' + 1)}{(y+1)} \right]^{\frac{1}{2}}, \tag{B.11}$$

¹⁷ The expression for C below differs by a factor of two from the expression in [12], but we believe that this expression is correct.

$$\begin{aligned}
R_{3\epsilon_x\epsilon_z}(x, y, z) &= \frac{(-1)^{\sigma+(\epsilon_x+\epsilon_z)/2}}{\pi} \left(\frac{(y+1)}{32(x+1)(z+1)} \right)^{\frac{1}{2}} \\
&\quad \cdot ((\epsilon_x(x+1) + \epsilon_z(z+1) + y + 2)(\epsilon_x(x+1) + \epsilon_z(z+1) + y) \\
&\quad \quad (\epsilon_x(x+1) + \epsilon_z(z+1) - y)(\epsilon_x(x+1) + \epsilon_z(z+1) - y - 2))^{\frac{1}{2}}, \\
R_{4\epsilon_x\epsilon_y\epsilon_z}(x, y, z) &= \frac{(-1)^{\sigma'+1}}{\pi} \text{sign}(\epsilon_x + \epsilon_y + \epsilon_z) \left(\frac{(\sigma'+1)(\sigma'-x)(\sigma'-y)(\sigma'-z)}{4(x+1)(y+1)(z+1)} \right)^{\frac{1}{2}} \\
&\quad \cdot ((\epsilon_x(x+1) + \epsilon_y(y+1) + \epsilon_z(z+1) + 2)(\epsilon_x(x+1) + \epsilon_y(y+1) + \epsilon_z(z+1) - 2))^{\frac{1}{2}}.
\end{aligned} \tag{B.12}$$

Here, the right-hand sides of the equations are defined to be non-zero only if the triangle inequality $|x - z| \leq y \leq x + z$ holds, and if $\sigma \equiv (x + y + z)/2$ (in R_1 and R_3) and $\sigma' \equiv (x + y + z + 1)/2$ (in R_2 and R_4) are integers. We also define $R_{3+} \equiv R_{3++} = R_{3--}$, $R_{3-} \equiv R_{3+-} = R_{3-+}$, $R_{4+} \equiv R_{4+++}$ and $R_{4-} \equiv R_{4++-}$.

B.3. Identities for sums of spherical harmonics

Using identities for 3j-symbols which may be found in [5], it is straightforward to derive expressions for sums over m , m' , and ϵ in various products of the spherical harmonic integrals. For our calculations, we require:

$$\begin{aligned}
\sum_{m's} B^{\alpha\bar{\alpha}\lambda} &= \frac{1}{\sqrt{2}\pi} (j_\alpha + 1)^2 \delta_{\lambda,0}, \\
\sum_{m's,\epsilon} D^{\alpha\bar{\alpha}\lambda} &= \frac{\sqrt{2}}{\pi} \delta_{\lambda,0} j_\alpha (j_\alpha + 2), \\
\sum_{m's,\epsilon} C^{\alpha\delta\gamma} C^{\bar{\gamma}\bar{\delta}\bar{\alpha}} &= -2R_2^2(j_\alpha, j_\delta, j_\gamma), \\
\sum_{m's,\epsilon's} D^{\alpha\beta\gamma} D^{\bar{\alpha}\bar{\beta}\bar{\gamma}} &= 2R_{3+}^2(j_\alpha, j_\gamma, j_\beta) + 2R_{3-}^2(j_\alpha, j_\gamma, j_\beta), \\
\sum_{m's,\epsilon's,j_\gamma} D^{\alpha\beta\gamma} D^{\bar{\alpha}\bar{\beta}\bar{\gamma}} &= \frac{2}{3\pi^2} j_\alpha (j_\alpha + 2) j_\beta (j_\beta + 2), \\
\sum_{m's} E^{\alpha\beta\gamma} E^{\bar{\alpha}\bar{\beta}\bar{\gamma}} &= R_{4\epsilon_\alpha\epsilon_\beta\epsilon_\gamma}^2(j_\alpha, j_\beta, j_\gamma).
\end{aligned} \tag{B.13}$$

Appendix C. Useful formulae for dimensional regularization

The following formulae are useful for our calculations in dimensional regularization of section 3.2:

$$\int \frac{d^d k}{(2\pi)^d} \frac{k^{2m}}{(k^2 + M^2)^n} = \frac{1}{M^{2n-2m-d}} \frac{1}{(4\pi)^{\frac{d}{2}}} \frac{\Gamma(n - m - \frac{d}{2}) \Gamma(m + \frac{d}{2})}{\Gamma(n) \Gamma(\frac{d}{2})}, \tag{C.1}$$

$$\zeta(1 + \epsilon) = \frac{1}{\epsilon} + \gamma + \mathcal{O}(\epsilon), \quad (\text{C.2})$$

$$\psi(z) \equiv \frac{\Gamma'(z)}{\Gamma(z)}, \quad (\text{C.3})$$

$$\psi(n) = -\gamma + \sum_{k=1}^{n-1} \frac{1}{k}, \quad (\text{C.4})$$

$$\psi\left(\frac{1}{2} + n\right) = -\gamma - 2 \ln(2) + 2 \sum_{k=1}^n \frac{1}{2k-1}. \quad (\text{C.5})$$

Appendix D. Regulating the Coulomb gauge

For our calculations here and in [5], we have used the Coulomb gauge, setting the divergence of the spatial gauge field to zero. In this gauge, the time component of the gauge field and the ghosts have no kinetic term, so their propagator contains a delta function. For diagrams containing A_0 or ghost loops, we then get a $\delta(0)$ factor. While this always cancels between the diagrams, one may be concerned that certain finite terms have been missed. Further, the singular propagators lead to ambiguities (which we did not encounter here) in certain calculations when the time derivative of the A_i propagator must be evaluated at $t = 0$.

To give an ambiguity-free definition of the Coulomb gauge, we can replace the strict $\vec{\nabla} \cdot \vec{A} = 0$ condition by a gauge-fixing action

$$S_{gf} = \int d^4x \operatorname{tr} \left(\frac{1}{2\xi} (\partial_0 A^0 + \xi \vec{\nabla} \cdot \vec{A})^2 \right), \quad (\text{D.1})$$

together with the corresponding ghost action

$$S_{gh} = \int d^4x \operatorname{tr} \left(\frac{1}{\xi} \partial_0 \bar{c} D_0 c + \partial_i \bar{c} D_i c \right). \quad (\text{D.2})$$

The Coulomb gauge may be defined as the $\xi \rightarrow \infty$ limit of this, but performing calculations at finite ξ avoids any $\delta(0)$ singularities (they show up as $\xi^{\frac{1}{2}}$ terms that cancel between the diagrams). In practice, we need only keep the $\xi^{\frac{1}{2}}$ and ξ^0 terms for each diagram. Using this procedure, we can verify that no additional finite terms arise in the cancellation of the $\delta(0)$'s in our calculation.

On the other hand, we have found that for certain other calculations, the naive Coulomb-gauge calculations can miss finite contributions. As an example, in the two-loop Casimir energy on the sphere, a diagram with two $\frac{1}{\xi} c A_0 c$ vertices gives a ξ -independent contribution that would be missed if we set $\xi = \infty$ from the start.

References

- [1] G. 't Hooft, “A planar diagram theory for strong interactions,” Nucl. Phys. B **72**, 461 (1974).
- [2] N. Beisert, G. Ferretti, R. Heise and K. Zarembo, “One-loop QCD spin chain and its spectrum,” Nucl. Phys. B **717**, 137 (2005) [arXiv:hep-th/0412029].
- [3] B. Sundborg, “The Hagedorn transition, deconfinement and $N = 4$ SYM theory,” Nucl. Phys. B **573**, 349 (2000) [arXiv:hep-th/9908001].
- [4] O. Aharony, J. Marsano, S. Minwalla, K. Papadodimas and M. Van Raamsdonk, “The Hagedorn / deconfinement phase transition in weakly coupled large N gauge theories,” Adv. Theor. Math. Phys. **8**, 603 (2004) [arXiv:hep-th/0310285].
- [5] O. Aharony, J. Marsano, S. Minwalla, K. Papadodimas and M. Van Raamsdonk, “A first order deconfinement transition in large N Yang-Mills theory on a small S^3 ,” Phys. Rev. D **71**, 125018 (2005) [arXiv:hep-th/0502149].
- [6] M. Spradlin and A. Volovich, “A pendant for Polya: The one-loop partition function of $N = 4$ SYM on $R \times S^3$,” Nucl. Phys. B **711**, 199 (2005) [arXiv:hep-th/0408178].
- [7] G. Leibbrandt and J. Williams, “Split Dimensional Regularization for the Coulomb Gauge,” Nucl. Phys. B **475**, 469 (1996) [arXiv:hep-th/9601046].
- [8] Y. H. Chen, R. J. Hsieh and C. I. Lin, “Split dimensional regularization for the temporal gauge,” arXiv:hep-th/9610165.
- [9] G. Leibbrandt, “The three-point function in split dimensional regularization in the Coulomb gauge,” Nucl. Phys. B **521**, 383 (1998) [arXiv:hep-th/9804109].
- [10] G. Heinrich and G. Leibbrandt, “Split dimensional regularization for the Coulomb gauge at two loops,” Nucl. Phys. B **575**, 359 (2000) [arXiv:hep-th/9911211].
- [11] M. Spradlin, M. Van Raamsdonk and A. Volovich, “Two-Loop Partition Function In The Planar Plane-Wave Matrix Model,” Phys. Lett. B **603**, 239 (2004) [arXiv:hep-th/0409178].
- [12] R. E. Cutkosky, “Harmonic functions and matrix elements for hyperspherical quantum field models,” J. Math. Phys. **25**, 939 (1984).